Journal of the Mechanics and Physics of Solids 60 (2012) 487–508

Contents lists available at SciVerse ScienceDirect

Journal of the Mechanics and Physics of Solids

journal homepage: www.elsevier.com/locate/jmps

Postbuckling analysis and its application to stretchable electronics

Yewang Su [a,1], Jian Wu [a,1], Zhichao Fan [a], Keh-Chih Hwang [a,*], Jizhou Song [b], Yonggang Huang [c,*], John A. Rogers [d]

[a] AML, Department of Engineering Mechanics, Tsinghua University, Beijing 100084, China
[b] Department of Mechanical and Aerospace Engineering, University of Miami, Coral Gables, FL 33124, USA
[c] Departments of Civil and Environmental Engineering and Mechanical Engineering, Northwestern University, Evanston, IL 60208, USA
[d] Department of Materials Science and Engineering, University of Illinois, Urbana, IL 61801, USA

ARTICLE INFO

Article history:
Received 13 September 2011
Received in revised form
12 November 2011
Accepted 19 November 2011
Available online 1 December 2011

Keywords:
Postbuckling
Stretchable electronics
Higher-order terms in curvature
Lateral buckling
Diagonal stretching

ABSTRACT

A versatile strategy for fabricating stretchable electronics involves controlled buckling of bridge structures in circuits that are configured into open, mesh layouts (i.e. islands connected by bridges) and bonded to elastomeric substrates. Quantitative analytical mechanics treatments of the responses of these bridges can be challenging, due to the range and diversity of possible motions. Koiter (1945) pointed out that the postbuckling analysis needs to account for all terms up to the 4th power of displacements in the potential energy. Existing postbuckling analyses, however, are accurate only to the 2nd power of displacements in the potential energy since they assume a linear displacement–curvature relation. Here, a systematic method is established for accurate postbuckling analysis of beams. This framework enables straightforward study of the complex buckling modes under arbitrary loading, such as lateral buckling of the island-bridge, mesh structure subject to shear (or twist) or diagonal stretching observed in experiments. Simple, analytical expressions are obtained for the critical load at the onset of buckling, and for the maximum bending, torsion (shear) and principal strains in the structure during postbuckling.

1. Introduction

Recent work suggests that it is possible to configure high performance electronic circuits, conventionally found in rigid, planar formats, into layouts that match the soft, curvilinear mechanics of biological tissues (Rogers et al., 2010). The resulting capabilities open up many application opportunities that cannot be addressed using established technologies. Examples include ultralight weight, rugged circuits (Kim et al., 2008a), flexible inorganic solar cells (Yoon et al., 2008) and LEDs (Park et al., 2009), soft, bio-integrated devices (Kim et al., 2010a, 2010b, 2011a, 2011b; Viventi et al., 2010), flexible displays (Crawford, 2005), eye-like digital cameras (Jin et al., 2004; Ko et al., 2008; Jung et al., 2011), structural health monitoring devices (Nathan et al., 2000), and electronic sensors for robotics (Someya et al., 2004; Mannsfeld et al., 2010; Takei et al., 2010) and even 'epidermal' electronics capable of mechanically invisible integration onto human skin (Kim et al., 2011b). Work in this area emphasizes mechanics and geometry, in systems that integrate hard materials for the active components of the devices with elastomers for the substrates and packaging components. (Rogers et al., 2010).

* Corresponding authors.
E-mail addresses: huangkz@tsinghua.edu.cn (K.-C. Hwang), y-huang@northwestern.edu (Y. Huang).
[1] Equal contribution to this paper.

0022-5096/$ - see front matter Crown Copyright © 2011 Published by Elsevier Ltd. All rights reserved.
doi:10.1016/j.jmps.2011.11.006

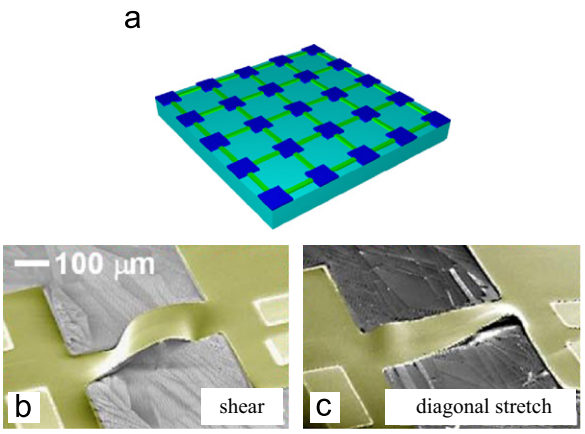

Fig. 1. (a) A schematic diagram of island-bridge, mesh structure in stretchable electronics; (b) SEM image (colorized for ease of viewing) of the island-bridge, mesh structure under shear; and (c) SEM image of the island-bridge, mesh structure under diagonal stretch.

A particularly successful strategy to stretchable electronics uses postbuckling of stiff, inorganic films on compliant, polymeric substrates (Bowden et al., 1998). Kim et al. (2008b) further improved by structuring the film into a mesh and bonding it to the substrate only at the nodes, as shown in Fig. 1a. Once buckled, the arc-shaped interconnects between the nodes can move freely out of the mesh plane to accommodate large applied strain (Song et al., 2009). The interconnects undergo complex buckling modes, such as lateral buckling, when subject to shear (Fig. 1b) or diagonal stretching (45° from the interconnects) (Fig. 1c). Different from Euler buckling, these complex buckling modes involve large torsion and out-of-plane bending. It is important to ensure the maximum strain in interconnects are below their fracture limit.

Koiter (1945, 1963, 2009) established a robust method for postbuckling analysis via energy minimization. The potential energy was expanded up to 4th power of displacement (from the non-buckled state), and the 3rd and 4th power terms actually governed the postbuckling behavior (Koiter, 1945). The existing analyses for postbuckling of plates (or shells), however, only account for the 1st power of the displacement in the curvature (von Karman and Tsien, 1941; Budiansky, 1973), which translates to the 2nd power of the displacement in the potential energy. This can be illustrated via a beam, whose curvature κ is approximately the 2nd order derivative of the deflection w, i.e., $\kappa=w''$. The bending energy is $(EI/2)\int w''^2dx$, where EI is the bending stiffness, and the integration is along the central axis x of the beam. The accurate expression of the curvature is $\kappa=w''/(1+w'^2)^{3/2}\approx w''[1-(3/2)w'^2]$, which gives bending energy $(EI/2)\int\kappa^2dx\approx(EI/2)\int w''^2(1-3w'^2)dx$. It is different from the approximate expression above by $(3EI/2)\int w''^2w'^2dx$, which is the 4th power of displacement, and may be important in the postbuckling analysis (Koiter, 1945).

The objective of this work is to establish a systematic method for postbuckling analysis of beams that may involve rather complex buckling modes such as lateral buckling of the island-bridge, mesh structure in stretchable electronics. It avoids the complex geometric analysis for lateral buckling (Timoshenko and Gere, 1961) and establishes a straightforward method to study any buckling mode. It accounts for all terms up to the 4th power of displacements in the potential energy, as suggested by Koiter (1945). Examples are given to show the importance of the 4th power of displacement, including the complex buckling patterns of the island-bridge, mesh structure for stretchable electronics (Fig. 1). Analytical expressions are obtained for the amplitude of, and the maximum strain in, buckled interconnects, which are important to the design of stretchable electronics.

2. Postbuckling analysis

2.1. Membrane strain and curvatures

Let Z denote the central axis of the beam before deformation. The unit vectors in the Cartesian coordinates (X,Y,Z) before deformation are $\boldsymbol{E}_i$ $(i=1,2,3)$. A point $\boldsymbol{X}=(0,0,Z)$ on the central axis moves to $\boldsymbol{X}+\boldsymbol{U}=(U_1,U_2,U_3+Z)$ after deformation, where $U_i(Z)$ $(i=1,2,3)$ are the displacements. The stretch along the axis is

$$\lambda=\sqrt{U_1'^2+U_2'^2+(1+U_3')^2}\approx 1+U_3'+\frac{1}{2}(U_1'^2+U_2'^2)-\frac{1}{2}U_3'(U_1'^2+U_2'^2), \tag{2.1}$$

where $()'=d()/dZ$, and terms higher than the 3rd power of displacement are neglected because their contribution to the potential energy are beyond the 4th power. The length dZ becomes λdZ after deformation.

The unit vector along the deformed central axis is $\boldsymbol{e}_3=d(\boldsymbol{X}+\boldsymbol{U})/(\lambda dZ)$. The other two unit vectors, $\boldsymbol{e}_1$ and $\boldsymbol{e}_2$, involve twist angle ϕ of the cross section around the central axis. Their derivatives are related to the curvature vector $\boldsymbol{\kappa}$ of the central

axis by Love (1927)

$$\frac{\boldsymbol{e}_i'}{\lambda}=\boldsymbol{\kappa}\times\mathbf{e}_i \quad (i=1,2,3), \tag{2.2}$$

where κ_1 and κ_2 are the curvatures in the $(\boldsymbol{e}_2,\boldsymbol{e}_3)$ and $(\boldsymbol{e}_1,\boldsymbol{e}_3)$ surfaces, respectively, and the twist curvature κ_3 is related to the twist angle ϕ of the cross section by

$$\kappa_3=\frac{\phi'}{\lambda}. \tag{2.3}$$

The unit vectors before and after deformation are related by the direction cosine a_{ij}

$$\boldsymbol{e}_i=a_{ij}\boldsymbol{E}_j \quad (i=1,2,3, \text{ summation over } j). \tag{2.4}$$

Eq. (2.2) gives 6 independent equations, while the orthonormal conditions $\boldsymbol{e}_i\cdot\boldsymbol{e}_j=\delta_{ij}$ give another 6. These 12 equations are solved to determine 9 direction cosines a_{ij} and 3 curvatures κ_i in terms of the displacements U_i and twist angle ϕ as

$$\{a_{ij}\}=\begin{Bmatrix}1&0&0\\0&1&0\\0&0&1\end{Bmatrix}+\begin{Bmatrix}0&\phi&-U_1'\\-\phi&0&-U_2'\\U_1'&U_2'&0\end{Bmatrix}+\begin{Bmatrix}-\frac{1}{2}(\phi^2+U_1'^2)&-\frac{1}{2}U_1'U_2'+\psi^{(2)}&U_1'U_3'-\phi U_2'\\-\frac{1}{2}U_1'U_2'-\psi^{(2)}&-\frac{1}{2}(\phi^2+U_2'^2)&U_2'U_3'+\phi U_1'\\-U_1'U_3'&-U_2'U_3'&-\frac{1}{2}(U_1'^2+U_2'^2)\end{Bmatrix}+\left\{a_{ij}^{(3)}\right\}, \tag{2.5}$$

where $\psi^{(2)}=\frac{1}{2}\int_0^Z(U_1'U_2''-U_1''U_2')dZ$ is the 2nd power of displacements, and $a_{ij}^{(3)}$ are the 3rd power of displacements and twist angle given in Appendix A. As to be shown in the next section, the work conjugate of bending moment and torque is $\hat{\boldsymbol{\kappa}}=\lambda\boldsymbol{\kappa}$, which is given in terms of the power of U_i and ϕ by

$$\{\hat{\kappa}_i\}=\begin{Bmatrix}-U_2''\\U_1''\\\phi'\end{Bmatrix}+\begin{Bmatrix}\phi U_1''+(U_2'U_3')'\\\phi U_2''-(U_1'U_3')'\\0\end{Bmatrix}+\{\hat{\kappa}_i^{(3)}\}, \tag{2.6}$$

where $\hat{\kappa}_i^{(3)}$ are the 3rd power of displacements given in Appendix A.

2.2. Force, bending moment and torque

Let $\boldsymbol{t}=t_i\boldsymbol{e}_i$ and $\boldsymbol{m}=m_i\boldsymbol{e}_i$ denote the forces and bending moment (and torque) in the cross section Z of the beam after deformation. Equilibrium of forces requires

$$\frac{\boldsymbol{t}'}{\lambda}+\boldsymbol{p}=0, \quad \text{or} \quad \begin{cases}t_1'-t_2\hat{\kappa}_3+t_3\hat{\kappa}_2+\lambda p_1=0\\t_2'+t_1\hat{\kappa}_3-t_3\hat{\kappa}_1+\lambda p_2=0\\t_3'-t_1\hat{\kappa}_2+t_2\hat{\kappa}_1+\lambda p_3=0\end{cases}, \tag{2.7}$$

where $\boldsymbol{p}$ is the distributed force on the beam (per unit length after deformation). Equilibrium of moments requires

$$\frac{\boldsymbol{m}'}{\lambda}+\boldsymbol{e}_3\times\boldsymbol{t}+\boldsymbol{q}=0, \quad \text{or} \quad \begin{cases}m_1'-m_2\hat{\kappa}_3+m_3\hat{\kappa}_2-\lambda t_2+\lambda q_1=0\\m_2'+m_1\hat{\kappa}_3-m_3\hat{\kappa}_1+\lambda t_1+\lambda q_2=0\\m_3'-m_1\hat{\kappa}_2+m_2\hat{\kappa}_1+\lambda q_3=0\end{cases}, \tag{2.8}$$

where $\boldsymbol{q}$ is the distributed moment on the beam (per unit length after deformation). Elimination of shear forces t_1 and t_2 from Eqs. (2.7) and (2.8) yields 4 equations for t_3 and $\boldsymbol{m}$. Principle of Virtual Work gives their work conjugates to be $\lambda-1$ and $\hat{\boldsymbol{\kappa}}$, respectively. For example, the virtual work of $\boldsymbol{m}$ is $\int\boldsymbol{m}\cdot\boldsymbol{\kappa}ds$, where $ds=\lambda dZ$ represents the integration along the central axis in the current (deformed) configuration. This integral can be equivalently written as $\int\boldsymbol{m}\cdot\hat{\boldsymbol{\kappa}}dZ$ in the initial (undeformed) configuration.

2.3. Onset of buckling and postbuckling

Let $\overset{\circ}{\boldsymbol{t}}$ and $\overset{\circ}{\boldsymbol{m}}$ denote the critical forces, bending moments and torque at the onset of buckling, at which the deformation is still small. The distributed force and moment at the onset of buckling are denoted by $\overset{\circ}{\boldsymbol{p}}$ and $\overset{\circ}{\boldsymbol{q}}$. Equilibrium Eqs. (2.7) and (2.8) at the onset of buckling are

$$\overset{\circ}{t}_i'+\overset{\circ}{p}_i=0 \quad (i=1,2,3), \tag{2.9}$$

$$\overset{\circ}{m}_1'-\overset{\circ}{t}_2+\overset{\circ}{q}_1=0, \quad \overset{\circ}{m}_2'+\overset{\circ}{t}_1+\overset{\circ}{q}_2=0, \quad \overset{\circ}{m}_3'+\overset{\circ}{q}_3=0. \tag{2.10}$$

The forces, bending moments and torque during postbuckling can be written as $\boldsymbol{t}=\overset{\circ}{\boldsymbol{t}}+\Delta\boldsymbol{t}$ and $\boldsymbol{m}=\overset{\circ}{\boldsymbol{m}}+\Delta\boldsymbol{m}$, where $\Delta\boldsymbol{t}$ and $\Delta\boldsymbol{m}$ are the changes beyond the onset of buckling. Equilibrium Eqs. (2.7) and (2.8) become

$$\begin{cases} \Delta t_1'-(\overset{\circ}{t}_2+\Delta t_2)\hat{\kappa}_3+(\overset{\circ}{t}_3+\Delta t_3)\hat{\kappa}_2+(\lambda p_1-\overset{\circ}{p}_1)=0 \\ \Delta t_2'+(\overset{\circ}{t}_1+\Delta t_1)\hat{\kappa}_3-(\overset{\circ}{t}_3+\Delta t_3)\hat{\kappa}_1+(\lambda p_2-\overset{\circ}{p}_2)=0, \\ \Delta t_3'-(\overset{\circ}{t}_1+\Delta t_1)\hat{\kappa}_2+(\overset{\circ}{t}_2+\Delta t_2)\hat{\kappa}_1+(\lambda p_3-\overset{\circ}{p}_3)=0 \end{cases} \tag{2.11}$$

$$\begin{cases} \Delta m_1'-(\overset{\circ}{m}_2+\Delta m_2)\hat{\kappa}_3+(\overset{\circ}{m}_3+\Delta m_3)\hat{\kappa}_2-[(\lambda-1)\overset{\circ}{t}_2+\lambda\Delta t_2]+(\lambda q_1-\overset{\circ}{q}_1)=0 \\ \Delta m_2'+(\overset{\circ}{m}_1+\Delta m_1)\hat{\kappa}_3-(\overset{\circ}{m}_3+\Delta m_3)\hat{\kappa}_1+[(\lambda-1)\overset{\circ}{t}_1+\lambda\Delta t_1]+(\lambda q_2-\overset{\circ}{q}_2)=0. \\ \Delta m_3'-(\overset{\circ}{m}_1+\Delta m_1)\hat{\kappa}_2+(\overset{\circ}{m}_2+\Delta m_2)\hat{\kappa}_1+(\lambda q_3-\overset{\circ}{q}_3)=0 \end{cases} \tag{2.12}$$

Elimination of Δt_1 and Δt_2 from Eqs. (2.11) and (2.12) yields 4 equations for Δt_3 and $\Delta\boldsymbol{m}$.

The linear elastic relations give Δt_3 and $\Delta\boldsymbol{m}$ in terms of the displacements U_i and twist angle ϕ by

$$\Delta t_3=EA(\lambda-1),\quad \Delta m_1=EI_1\hat{\kappa}_1,\quad \Delta m_2=EI_2\hat{\kappa}_2,\quad \Delta m_3=C\hat{\kappa}_3, \tag{2.13}$$

where EA is the tensile stiffness, EI_1 and EI_2 are the bending stiffness, and C is the torsion stiffness. Substitution of Eq. (2.13) into Eqs. (2.11) and (2.12) leads to four ordinary differential equations (ODEs) for U_i and ϕ.

Examples in the following sections show that the buckling analysis (both onset of buckling and postbuckling) is straightforward even for complex buckling modes such as the island-bridge, mesh structure in stretchable electronics in Section 5. It is much simpler than the existing analysis for the onset of buckling, which works only for relatively simple buckling modes (Timoshenko and Gere, 1961). It is also more accurate than the existing postbuckling analysis, which neglects the 2nd and 3rd power of displacements in the curvature (von Karman and Tsien, 1941; Budiansky, 1973).

3. Euler-type buckling

Consider a beam of length L with one end clamped and the other simply supported. The beam is subject to uniaxial compression force P. There are no distributed force and moment in the beam, $\boldsymbol{p}=\boldsymbol{q}=0$. Let $\overset{\circ}{P}$ denote the critical compression at the onset of buckling (to be determined), and ΔP the change of P beyond $\overset{\circ}{P}$. The forces, bending moments and torque at the onset of buckling are $\overset{\circ}{t}_1=\overset{\circ}{t}_2=0$, $\overset{\circ}{t}_3=-\overset{\circ}{P}$ and $\overset{\circ}{\boldsymbol{m}}=0$. Without losing generality it is assumed the bending stiffness $EI_1>EI_2$ such that the beam buckles within the (X,Z) plane (Fig. 2). This gives $U_2=\phi=0$, and therefore $\hat{\kappa}_1=\hat{\kappa}_3=0$ from Eq. (2.6) and $\Delta m_1=\Delta m_3=0$ from Eq. (2.13). Eqs. (2.11) and (2.12) give $\Delta t_2=0$, and

$$\Delta t_1'+(-\overset{\circ}{P}+\Delta t_3)\hat{\kappa}_2=0,\quad \Delta t_3'-\Delta t_1\hat{\kappa}_2=0,\quad \Delta m_2'+\lambda\Delta t_1=0. \tag{3.1}$$

Elimination of Δt_1, together with the linear elastic relation Eq. (2.13), give

$$EI_2\left(\frac{\hat{\kappa}_2'}{\lambda}\right)'+\left[\overset{\circ}{P}-EA(\lambda-1)\right]\hat{\kappa}_2=0,\quad (EA\lambda^2+EI_2\hat{\kappa}_2^2)'=0. \tag{3.2}$$

Eq. (2.6) gives $\hat{\kappa}_2$ on the order of U_1. Its substitution into Eq. (3.1) gives Δt_1 and Δm_2 on the order of U_1, and Δt_3 on the order of $(U_1)^2$. The linear elastic relation $\Delta t_3=EA(\lambda-1)$ in Eq. (2.13) and the stretch λ in Eq. (2.1) suggest U_3 on the order of $(U_1)^2$

$$U_3\sim(U_1)^2. \tag{3.3}$$

The stretch in Eq. (2.1) becomes

$$\lambda=1+U_3'+\frac{1}{2}U_1'^2+O\left[(U_1)^4\right]. \tag{3.4}$$

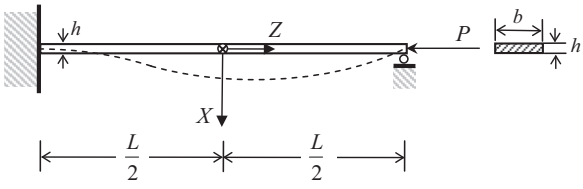

Fig. 2. Illustration of beam buckling under compression, with one end clamped and the other simply supported.

The only non-zero curvature obtained from Eq. (2.6) and $\hat{\kappa}_i^{(3)}$ in Appendix A is

$$\hat{\kappa}_2 = U_1'' - \underline{\left(U_1' U_3' + \frac{1}{3}U_1'^3\right)'} + O\left[(U_1)^5\right], \tag{3.5}$$

where the underlined are the higher-order terms in the curvature neglected by von Karman and Tsien (1941) and Budiansky (1973). (Their curvatures neglected the 2nd and 3rd power of displacements in the postbuckling analysis of plates.) Substitution of Eqs. (3.4) and (3.5) into (3.2) gives two equations for U_1 and U_3

$$\left[U_1'''\left(1-U_3'-\frac{1}{2}U_1'^2\right)\right]' + \frac{\overset{o}{P}}{EI_2}U_1'' - \frac{EA}{EI_2}U_1''\left(U_3'+\frac{1}{2}U_1'^2\right) - \underline{\left(U_1'U_3'+\frac{1}{3}U_1'^3\right)'''} - \frac{\overset{o}{P}}{EI_2}\underline{\left(U_1'U_3'+\frac{1}{3}U_1'^3\right)'} + O\left[(U_1)^5\right] = 0, \tag{3.6}$$

$$\left[\frac{EA}{EI_2}(2U_3'+U_1'^2)+U_1''^2\right]' + O\left[(U_1)^4\right] = 0. \tag{3.7}$$

The boundary conditions at the clamped end ($Z=-L/2$, Fig. 2) are

$$U_1 = U_1' = U_3 = 0 \quad \text{at} \quad Z = -L/2 \tag{3.8}$$

The vanishing displacement and bending moment $\Delta m_2 = 0$ at the simply supported end ($Z=L/2$) gives

$$U_1 = U_1'' - \underline{\left(U_1'U_3'+\frac{1}{3}U_1'^3\right)'} + O\left[(U_1)^5\right] = 0 \quad \text{at} \quad Z = L/2, \tag{3.9}$$

where Eqs. (2.13) and (3.5) have been used. The traction at this end is $\Delta t_1 \boldsymbol{e}_1 + (-\overset{o}{P}+\Delta t_3)\boldsymbol{e}_3$; its component along the axial direction $\boldsymbol{E}_3$ in the initial (undeformed) configuration must be $-(\overset{o}{P}+\Delta P)$, which gives

$$\Delta t_1 \boldsymbol{e}_1 \cdot \boldsymbol{E}_3 + (-\overset{o}{P}+\Delta t_3)\boldsymbol{e}_3 \cdot \boldsymbol{E}_3 = -(\overset{o}{P}+\Delta P), \quad \text{at} \quad Z = L/2, \tag{3.10}$$

or using the direction cosines a_{ij} in Eq. (2.5) (and $a_{ij}^{(3)}$ in Appendix A)

$$-\Delta t_1 U_1' - \overset{o}{P}\left(1-\frac{1}{2}U_1'^2\right) + \Delta t_3 = -(\overset{o}{P}+\Delta P) + O\left[(U_1)^4\right] \quad \text{at} \quad Z = L/2 \tag{3.10a}$$

Elimination of Δt_1 and Δt_3 in the above equation via Eqs. (3.1), (2.13), (3.4) and (3.5) gives

$$U_1'U_1''' + \frac{\overset{o}{P}}{2EI_2}U_1'^2 + \frac{EA}{EI_2}\left(U_3'+\frac{1}{2}U_1'^2\right) + \frac{\Delta P}{EI_2} + O\left[(U_1)^4\right] = 0 \quad \text{at} \quad Z = L/2. \tag{3.11}$$

The perturbation method is used to solve ODEs (3.6) and (3.7) with boundary conditions (3.8), (3.9) and (3.11). Let a be the ratio of the maximum deflection $U_{1\max}$ to the beam length L; a is small such that displacements U_1 and U_3 are expressed as the power series of a. It can be shown that U_1 and U_3 correspond to the odd and even powers of a, respectively, and can be written as

$$\begin{aligned} U_1 &= aU_{1(0)} + a^3U_{1(1)} + \ldots \\ U_3 &= a^2U_{3(0)} + \ldots, \end{aligned} \tag{3.12}$$

where terms higher than the 3rd power of displacement (i.e., higher than a^3) are neglected in the postbuckling analysis. Similarly, ΔP is on the order of a^2, and can be written as

$$\Delta P = a^2 \Delta P_{(0)} + \ldots. \tag{3.13}$$

Substitution of Eqs. (3.12) and (3.13) into Eqs. (3.6)–(3.9) and (3.11) gives

$$\begin{cases} \left(U_{1(0)}'' + \frac{\overset{o}{P}}{EI_2}U_{1(0)}\right)'' = 0 \\ U_{1(0)}\big|_{Z=-L/2} = U_{1(0)}'\big|_{Z=-L/2} = U_{1(0)}\big|_{Z=L/2} = U_{1(0)}''\big|_{Z=L/2} = 0 \end{cases}, \tag{3.14}$$

$$\begin{cases} \left(2U_{3(0)}' + U_{1(0)}'^2 + \frac{EI_2}{EA}U_{1(0)}''^2\right)' = 0 \\ U_{3(0)}\big|_{Z=-L/2} = \left(U_{3(0)}' + \frac{1}{2}U_{1(0)}'^2 + \frac{EI_2}{EA}U_{1(0)}'U_{1(0)}''' + \frac{\overset{o}{P}}{2EA}U_{1(0)}'^2 + \frac{\Delta P_{(0)}}{EA}\right)\Big|_{Z=L/2} \end{cases} = 0 \tag{3.15}$$

for the leading powers of a, and

$$\begin{cases} \left(U''_{1(1)}+\frac{\overset{o}{P}}{EI_2}U_{1(1)}\right)''=\left[U'''_{1(0)}\left(U'_{3(0)}+\frac{1}{2}U'^2_{1(0)}\right)\right]'+\frac{EA}{EI_2}U''_{1(0)}\left(U'_{3(0)}+\frac{1}{2}U'^2_{1(0)}\right) \\ \quad+\underline{\left(U'_{1(0)}U'_{3(0)}+\frac{1}{3}U'^3_{1(0)}\right)'''}+\frac{\overset{o}{P}}{EI_2}\underline{\left(U'_{1(0)}U'_{3(0)}+\frac{1}{3}U'^3_{1(0)}\right)'} \\ U_{1(1)}|_{Z=-L/2}=U'_{1(1)}|_{Z=-L/2}=U_{1(1)}|_{Z=L/2}=\left[U''_{1(1)}-\left(U'_{1(0)}U'_{3(0)}+\frac{1}{3}U'^3_{1(0)}\right)'\right]\Big|_{Z=L/2}=0 \end{cases} \tag{3.16}$$

for the next power of a, where the underline represents the higher-order terms neglected in the existing postbuckling analysis.

Eq. (3.14) constitutes an eigenvalue problem for $U_{1(0)}$. The critical buckling load is the eigenvalue, and is given by

$$\overset{o}{P}=\frac{k^2EI_2}{L^2}=\frac{20.19EI_2}{L^2}, \tag{3.17}$$

where $k=4.493$ is the smallest positive root of the equation

$$\tan k=k. \tag{3.18}$$

The corresponding buckling mode is

$$U_{1(0)}=\frac{k(L-2Z)}{4\pi}-\frac{L\sin\left(k\frac{L-2Z}{2L}\right)}{2\pi\cos k}, \tag{3.19}$$

and its maximum is L. Eq. (3.15) gives $U'_{3(0)}$ as

$$U'_{3(0)}=-\frac{k^2}{8\pi^2}\left[\frac{\cos\left(k\frac{L-2Z}{2L}\right)}{\cos k}-1\right]^2+\frac{k^2\overset{o}{P}}{8\pi^2EA}\left[\frac{\cos^2\left(k\frac{L-2Z}{2L}\right)}{\cos^2 k}-1\right]-\frac{\Delta P_{(0)}}{EA}. \tag{3.20}$$

Its integration, together with $U_{3(0)}|_{Z=-L/2}=0$ in Eq. (3.15), gives $U_{3(0)}$.

The higher-order displacement $U_{1(1)}$ could be obtained from Eq. (3.16). However, ΔP can be determined directly without solving $U_{1(1)}$. This is because $\{U''_{1(1)}+[\overset{o}{P}/(EI_2)]U_{1(1)}\}''$ in Eq. (3.16) is orthogonal to $U_{1(0)}$

$$\int_{-L/2}^{L/2}\left\{U''_{1(1)}+[\overset{o}{P}/(EI_2)]U_{1(1)}\right\}''U_{1(0)}dZ=0$$

(also shown in Appendix A). Substitution of $\{U''_{1(1)}+[\overset{o}{P}/(EI_2)]U_{1(1)}\}''$ in Eq. (3.16) into the above integral gives the equation for ΔP

$$\int_{-L/2}^{L/2}\left\{\begin{array}{l}\left[U'''_{1(0)}\left(U'_{3(0)}+\frac{1}{2}U'^2_{1(0)}\right)\right]'+\frac{EA}{EI_2}U''_{1(0)}\left(U'_{3(0)}+\frac{1}{2}U'^2_{1(0)}\right)\\ +\underline{\left(U'_{1(0)}U'_{3(0)}+\frac{1}{3}U'^3_{1(0)}\right)'''}+\frac{\overset{o}{P}}{EI_2}\underline{\left(U'_{1(0)}U'_{3(0)}+\frac{1}{3}U'^3_{1(0)}\right)'}\end{array}\right\}U_{1(0)}dZ=0. \tag{3.21}$$

This gives

$$\Delta P_{(0)}=\overset{o}{P}\frac{k^2}{288\pi^2}\frac{9k^2-25-(27k^2-3)\frac{\overset{o}{P}}{EA}-\underline{\left(20+12\frac{\overset{o}{P}}{EA}\right)}}{1-\overset{o}{P}/(EA)}\approx\overset{o}{P}\frac{k^2(9k^2-25-\underline{20})}{288\pi^2}, \tag{3.22}$$

where the underline represents the contribution neglected in the existing postbuckling analysis, without which the existing postbuckling analysis would give $\Delta P_{(0)}=1.113\overset{o}{P}$, which is 15% larger than $\Delta P_{(0)}=0.971\overset{o}{P}$ obtained from Eq. (3.22).

The compression force P is then related to the maximum deflection $U_{1\max}$ during postbuckling by

$$P\approx\overset{o}{P}+a^2\overset{o}{P}\frac{k^2(9k^2-25-\underline{20})}{288\pi^2}=\overset{o}{P}\left[1+\frac{k^2(9k^2-25-\underline{20})}{288\pi^2}\left(\frac{U_{1\max}}{L}\right)^2\right], \tag{3.23}$$

where $a=U_{1\max}/L$ has been used. The critical compressive strain at the onset of buckling, $-\overset{o}{P}/(EA)=-20.19EI_2/(EAL^2)$, is negligible. The applied (compressive) strain during postbuckling is

$$\varepsilon_{applied}=\frac{U_3|_{Z=L/2}-U_3|_{Z=-L/2}}{L}=\frac{a^2}{L}\int_{-L/2}^{L/2}U'_{3(0)}dZ\approx-\frac{k^4}{16\pi^2}\left(\frac{U_{1\max}}{L}\right)^2=-2.58\left(\frac{U_{1\max}}{L}\right)^2. \tag{3.24}$$

The compression force P is then related to the applied (compressive) strain $\varepsilon_{applied}$ by

$$P \approx \overset{o}{P}\left(1+\frac{9k^2-25-20}{18k^2}|\varepsilon_{applied}|\right)=\overset{o}{P}(1+0.3762|\varepsilon_{applied}|), \tag{3.25}$$

while the existing postbuckling analysis would give $P \approx \overset{o}{P}(1+0.4312|\varepsilon_{applied}|)$.

The maximum membrane strain in the beam is $-\overset{o}{P}/(EA)\cdot\{1+O[(U_{1\max}/L)^2]\}$, which is on the order of h^2/L^2, where h is the beam height. It is negligible as compared to the bending strain given below for the maximum deflection $U_{1\max}$ much larger than h. The maximum bending strain in the beam is given by

$$\varepsilon_{\max}=\frac{h}{2}\max|U_1''|=4.603\frac{h}{L}\sqrt{|\varepsilon_{applied}|}, \tag{3.26}$$

which is much smaller than the applied strain for $U_{1\max} \gg h$.

4. Lateral buckling

In general, the following orders of displacement and rotation increments hold during postbuckling:

(i) The increment of axial displacement U_3 is always 2nd order;
(ii) The deflection and rotations increments during postbuckling are 1st order if these increments are zero prior to the onset of buckling (e.g., U_1 and ϕ in this section);
(iii) The deflection and rotations increments during postbuckling are 2nd order if these increments are not zero prior to the onset of buckling (e.g., U_2 in this section).

Fig. 3 shows a beam of length L with the left end clamped and the right end subject to a shear force P in the Y direction without any rotation. Let Z denote the central axis of the beam before deformation, and with $Z=0$ at the beam center. The beam buckles out of the Y–Z plane (i.e., lateral buckling) when the shear force P reaches the critical buckling load $\overset{o}{P}$ (to be

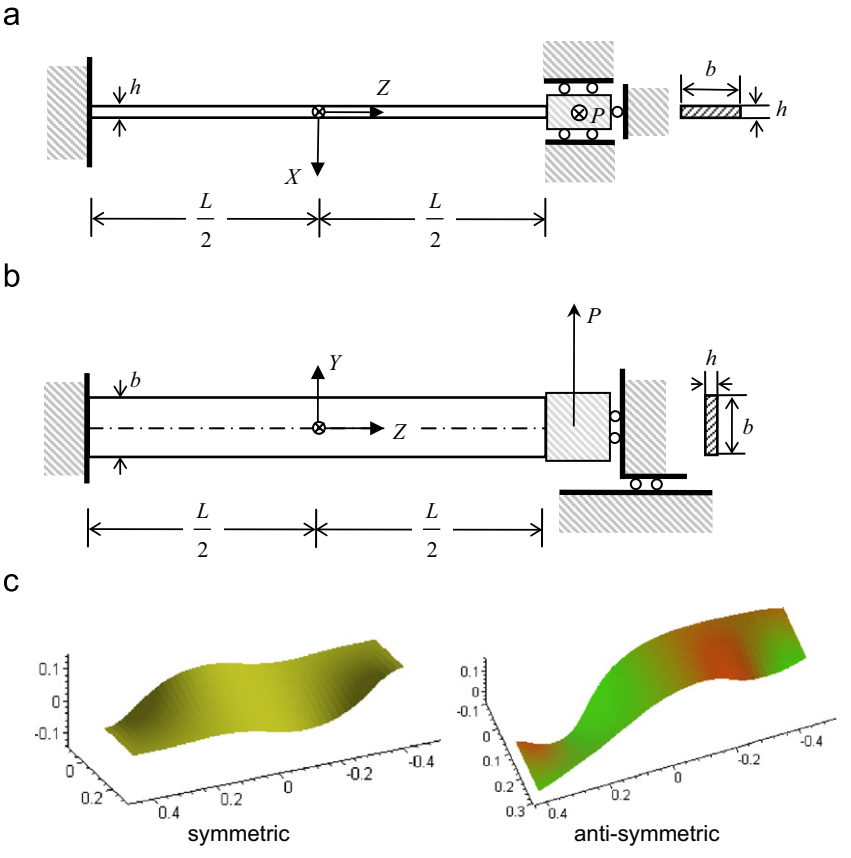

Fig. 3. Illustration of lateral buckling of a beam under shear along the thick direction ($b \gg h$) of the cross section; (a) view along the direction of shear; (b) view normal to the direction of shear; and (c) the symmetric and anti-symmetric buckling modes.

determined). As to be shown at the end of Section 4, this represents a special case of the island-bridge, mesh structure in stretchable electronics (Kim et al., 2008b).

4.1. Equations for postbuckling analysis

There are no distributed force and moment, $\boldsymbol{p}=\boldsymbol{q}=0$. The force, bending moment and torque in the beam prior to the onset of buckling are

$$\overset{o}{t}_1=\overset{o}{t}_3=\overset{o}{m}_2=\overset{o}{m}_3=0,\quad \overset{o}{t}_2=\overset{o}{P},\quad \overset{o}{m}_1=\overset{o}{P}Z\quad \text{for}\quad -\frac{L}{2}\le Z\le\frac{L}{2}. \tag{4.1}$$

Let $\Delta P=P-\overset{o}{P}$ denote the change of shear force during postbuckling. Only the displacements along Z and Y directions are not zero prior to the onset of buckling. Therefore the displacement U_1 and rotation ϕ during postbuckling are 1st order, and displacements U_2 and U_3 are 2nd order, i.e.,

$$\phi\sim U_1,\quad U_2\sim U_3\sim (U_1)^2. \tag{4.2}$$

The stretch in Eq. (2.1) becomes

$$\lambda=1+U_3'+\frac{1}{2}U_1'^2+O\left[(U_1)^4\right]. \tag{4.3}$$

Eq. (2.6) and $\hat{\kappa}_i^{(3)}$ in Appendix A give the curvatures

$$\begin{aligned}&\hat{\kappa}_1=-U_2''+\underline{\phi U_1''}+O\left[(U_1)^4\right],\\ &\hat{\kappa}_2=U_1''+\underline{\phi U_2''-(U_1'U_3')'-\frac{1}{2}\phi^2U_1''-\frac{1}{3}(U_1'^3)'}+O\left[(U_1)^5\right],\quad \hat{\kappa}_3=\phi',\end{aligned} \tag{4.4}$$

where the underlined are the higher-order terms in the curvatures neglected in the existing postbuckling analysis (von Karman and Tsien, 1941; Budiansky, 1973). Substitution Eqs. (4.1)–(4.4) into Eqs. (2.11)–(2.13) gives the ODEs for $\boldsymbol{U}$ and ϕ

$$C\phi''+(EI_1-EI_2)U_1''(U_2''-\underline{\phi U_1''})-\overset{o}{P}Z\left[U_1''+\underline{\phi U_2''-(U_1'U_3')'-\frac{1}{2}\phi^2U_1''-\frac{1}{3}(U_1'^3)'}\right]+O\left[(U_1)^5\right]=0, \tag{4.5}$$

$$\begin{aligned}&EI_2\left\{U_1^{(4)}-U_1'''\left(U_3'+\frac{1}{2}U_1'^2\right)'-\phi'^2U_1''+\left[\underline{\phi U_2''-(U_1'U_3')'-\frac{1}{2}\phi^2U_1''-\frac{1}{3}(U_1'^3)'}\right]''\right\}\\ &\quad -EI_1\left[\phi''(U_2''-\underline{\phi U_1''})+2\phi'(U_2''-\underline{\phi U_1''})'\right]+C\left[\phi''(U_2''-\underline{\phi U_1''})+\phi'(U_2''-\underline{\phi U_1''})'+\phi'^2U_1''\right]\\ &\quad -EAU_1''\left(U_3'+\frac{1}{2}U_1'^2\right)+\overset{o}{P}\phi'+(\overset{o}{P}Z\phi')'-\overset{o}{P}Z\phi'\left(U_3'+\frac{1}{2}U_1'^2\right)'+O\left[(U_1)^5\right]=0,\end{aligned} \tag{4.6}$$

$$EI_1(U_2''-\underline{\phi U_1''})''+EI_2(\phi''U_1''+2\phi'U_1''')-C(\phi'U_1'')'+\overset{o}{P}\left(U_3'+\frac{1}{2}U_1'^2\right)'+\overset{o}{P}Z\phi'^2+O\left[(U_1)^4\right]=0, \tag{4.7}$$

$$\left[EA\left(U_3'+\frac{1}{2}U_1'^2\right)+\frac{1}{2}EI_2U_1''^2\right]'-\overset{o}{P}(U_2''-\underline{\phi U_1''})+\overset{o}{P}Z\phi'U_1''+O\left[(U_1)^4\right]=0. \tag{4.8}$$

The increments of axial force Δt_3 and bending moment and torque $\Delta\boldsymbol{m}$ can be obtained from Eqs. (2.13), (4.3) and (4.4). The shear forces, needed in the boundary conditions, are given by

$$\begin{aligned}&\lambda\Delta t_1=-EI_2\left[U_1''+\underline{\phi U_2''-(U_1'U_3')'-\frac{1}{2}\phi^2U_1''-\frac{1}{3}(U_1'^3)'}\right]'+(EI_1-C)\phi'(U_2''-\underline{\phi U_1''})-\overset{o}{P}Z\phi'+O\left[(U_1)^5\right]\\ &\lambda\Delta t_2=-EI_1(U_2''-\underline{\phi U_1''})'-(EI_2-C)\phi'U_1''-\overset{o}{P}\left(U_3'+\frac{1}{2}U_1'^2\right)+O\left[(U_1)^4\right].\end{aligned} \tag{4.9}$$

The displacements U_2 and U_3 at the left end are zero

$$U_2=U_3=0\quad \text{at}\quad Z=-L/2. \tag{4.10}$$

The boundary conditions at the two ends are zero displacement

$$U_1=0\quad \text{at}\quad Z=\pm L/2 \tag{4.11}$$

and zero rotation, $\boldsymbol{e}_i=\boldsymbol{E}_i$ $(i=1,2,3)$, and therefore direction cosines $a_{ij}=\delta_{ij}$, which are expressed in terms of displacements and rotation as

$$U_1'=0,\quad U_2'=0,\quad \phi+\psi^{(2)}+\psi^{(3)}=0\quad \text{at}\quad Z=\pm L/2, \tag{4.12}$$

where

$$\psi^{(2)}=\frac{1}{2}\int_0^Z(U_1'U_2''-U_1''U_2')dZ$$

given after Eq. (2.5) is in the order of $O[(U_1)^3]$, and $\psi^{(3)}$ given in Appendix A is also in the order of $O[(U_1)^3]$. The traction condition at the right end $Z=L/2$ is

$$\Delta t_2=\Delta P,\quad \Delta t_3=0\quad \text{at}\quad Z=L/2. \tag{4.13}$$

Substitution of Δt_2 in Eq. (4.9) and Δt_3 from Eqs. (2.13) and (4.3) into the above equation gives

$$\begin{aligned}&U_3'+O\left[(U_1)^4\right]=0\\&(U_2''-\underline{\phi U_1''})'+\frac{EI_2-C}{EI_1}\phi' U_1''+\frac{\overset{\circ}{P}}{EI_1}U_3'+\frac{\Delta P}{EI_1}+O\left[(U_1)^4\right]=0\quad \text{at}\quad Z=L/2.\end{aligned} \tag{4.14}$$

4.2. Perturbation method

The perturbation method is used to solve the ODEs (4.5)–(4.8) with boundary conditions (4.10)–(4.12) and (4.14). Let a denote a small non-dimensional parameter, such as the ratio of the maximum deflection $U_{1\max}$ to the beam length L or the maximum twist ϕ. The displacements and rotation are expanded to the power series of a, with ϕ and U_1 to the odd powers of a, and U_2 and U_3 to the even powers of a

$$\begin{aligned}&\phi=a\phi_{(0)}+a^3\phi_{(1)}+\ldots\\&U_1=aU_{1(0)}+a^3U_{1(1)}+\ldots\\&U_2=a^2U_{2(0)}+\ldots\\&U_3=a^2U_{3(0)}+\ldots,\end{aligned} \tag{4.15}$$

where terms higher than the 3rd power of displacement [i.e., $o(a^3)$] are neglected in the postbuckling analysis. Similarly, ΔP is in the order of a^2, and can be written as

$$\Delta P=a^2\Delta P_{(0)}+\ldots. \tag{4.16}$$

Substitution of the above two equations into the ODEs and boundary conditions gives

$$\begin{cases}C\phi_{(0)}''-\overset{\circ}{P}ZU_{1(0)}''=0\\EI_2U_{1(0)}^{(4)}+\overset{\circ}{P}\phi_{(0)}'+(\overset{\circ}{P}Z\phi_{(0)}')'=0\\\phi_{(0)}\big|_{Z=\pm L/2}=U_{1(0)}\big|_{Z=\pm L/2}=U_{1(0)}'\big|_{Z=\pm L/2}=0\end{cases}, \tag{4.17}$$

$$\begin{cases}EI_1(U_{2(0)}''-\underline{\phi_{(0)}U_{1(0)}''})''+EI_2(\phi_{(0)}''U_{1(0)}''+2\phi_{(0)}'U_{1(0)}''')-C(\phi_{(0)}'U_{1(0)}'')'+\overset{\circ}{P}\left(U_{3(0)}'+\frac{1}{2}U_{1(0)}'^2\right)'+\overset{\circ}{P}Z\phi_{(0)}'^2=0\\\left[EA\left(U_{3(0)}'+\frac{1}{2}U_{1(0)}'^2\right)+\frac{1}{2}EI_2U_{1(0)}''^2\right]'-\overset{\circ}{P}(U_{2(0)}''-\underline{\phi_{(0)}U_{1(0)}''})+\overset{\circ}{P}Z\phi_{(0)}'U_{1(0)}''=0\\U_{2(0)}\big|_{Z=-L/2}=U_{3(0)}\big|_{Z=-L/2}=U_{2(0)}'\big|_{Z=\pm L/2}=U_{3(0)}'\big|_{Z=L/2}=0\\\left[(U_{2(0)}''-\underline{\phi_{(0)}U_{1(0)}''})'+\frac{EI_2-C}{EI_1}\phi_{(0)}'U_{1(0)}''+\frac{1}{EI_1}\overset{\circ}{P}U_{3(0)}'\right]_{Z=L/2}=-\frac{\Delta P_{(0)}}{EI_1}\end{cases} \tag{4.18}$$

for the leading powers of a, and

$$\begin{cases}C\phi_{(1)}''-\overset{\circ}{P}ZU_{1(1)}''=-(EI_1-EI_2)U_{1(0)}''(U_{2(0)}''-\underline{\phi_{(0)}U_{1(0)}''})+\overset{\circ}{P}Z\left[\underline{\phi_{(0)}U_{2(0)}''-(U_{1(0)}'U_{3(0)}')'-\frac{1}{2}\phi_{(0)}^2U_{1(0)}''-\frac{1}{3}(U_{1(0)}'^3)'}\right]\\EI_2U_{1(1)}^{(4)}+\overset{\circ}{P}\phi_{(1)}'+(\overset{\circ}{P}Z\phi_{(1)}')'=EI_2\left\{\begin{array}{l}U_{1(0)}'''\left(U_{3(0)}'+\frac{1}{2}U_{1(0)}'^2\right)'+\phi_{(0)}'^2U_{1(0)}''\\-\left[\underline{\phi_{(0)}U_{2(0)}''-(U_{1(0)}'U_{3(0)}')'-\frac{1}{2}\phi_{(0)}^2U_{1(0)}''-\frac{1}{3}(U_{1(0)}'^3)'}\right]''\end{array}\right\}\\\quad+EI_1\left[\phi_{(0)}''(U_{2(0)}''-\underline{\phi_{(0)}U_{1(0)}''})+2\phi_{(0)}'(U_{2(0)}''-\underline{\phi_{(0)}U_{1(0)}''})'\right]\\\quad-C\left[\phi_{(0)}''(U_{2(0)}''-\underline{\phi_{(0)}U_{1(0)}''})+\phi_{(0)}'(U_{2(0)}''-\underline{\phi_{(0)}U_{1(0)}''})'+\phi_{(0)}'^2U_{1(0)}''\right]\\\quad+EAU_{1(0)}''\left(U_{3(0)}'+\frac{1}{2}U_{1(0)}'^2\right)+\overset{\circ}{P}Z\phi_{(0)}'\left(U_{3(0)}'+\frac{1}{2}U_{1(0)}'^2\right)'\\[\phi_{1(1)}+\psi_{(0)}^{(2)}+\psi_{(0)}^{(3)}]\big|_{Z=\pm L/2}=U_{1(1)}\big|_{Z=\pm L/2}=U_{1(1)}'\big|_{Z=\pm L/2}=0\end{cases} \tag{4.19}$$

for the next power of a, where

$$\psi_{(0)}^{(2)}=\frac{1}{2}\int_0^Z(U_{1(0)}'U_{2(0)}''-U_{1(0)}''U_{2(0)}')dZ\quad\text{and}\quad\psi_{(0)}^{(3)}=-\frac{1}{4}\phi_{(0)}\left(\frac{2}{3}\phi_{(0)}^2+U_{1(0)}'^2\right).$$

Eq. (4.17) constitutes an eigenvalue problem for $\phi_{(0)}$ and $U_{1(0)}$. Elimination of $U_{1(0)}$ yields the equation for $\phi_{(0)}$

$$\frac{d}{dZ}\left[\phi'''_{(0)}-\frac{2}{Z}\phi''_{(0)}+\frac{(\overset{o}{P}Z)^2}{EI_2C}\phi'_{(0)}\right]=0. \tag{4.20}$$

It has two sets of solutions, corresponding to even and odd functions of Z, respectively, which are called symmetric and anti-symmetric buckling modes in Sections 4.3 and 4.4. It can be shown that $U_{1(0)}$ is odd for an even $\phi_{(0)}$, and $U_{1(0)}$ is even when $\phi_{(0)}$ is odd.

For the beam with a narrow cross section such that $EI_1 \gg EI_2, C$ as in experiments, Eq. (4.18) can be significantly simplified by neglecting $EI_2/(EI_1)$ and $C/(EI_1)$

$$\begin{cases}(U''_{2(0)}-\underline{\phi_{(0)}U''_{1(0)}})''=0\\ U_{2(0)}\big|_{Z=-L/2}=U'_{2(0)}\big|_{Z=\pm L/2}=(U''_{2(0)}-\underline{\phi_{(0)}U''_{1(0)}})'\big|_{Z=L/2}=0\end{cases}$$

$$\begin{cases}\left(U'_{3(0)}+\frac{1}{2}U'^2_{1(0)}\right)'=0\\ U_{3(0)}\big|_{Z=-L/2}=U'_{3(0)}\big|_{Z=L/2}=0,\end{cases} \tag{4.18a}$$

where the deformation at the onset of buckling is negligible since $\overset{o}{P}$ and $\Delta P_{(0)}$ are proportional to $\sqrt{EI_2C}$ (to be shown in Sections 4.3 and 4.4) and the bridge length L is much larger than the cross section dimension (e.g., thickness). The above equation, together with $\phi_{(0)}$ and $U_{1(0)}$ being opposite even or odd functions, give $U''_{2(0)}=\underline{\phi_{(0)}U''_{1(0)}}$ and $U'_{3(0)}=-U'^2_{1(0)}/2$. Its solution is

$$\begin{aligned}U_{2(0)}&=-Z\int_Z^{L/2}\underline{\phi_{(0)}U''_{1(0)}}dZ_1-\int_0^Z Z_1\underline{\phi_{(0)}U''_{1(0)}}dZ_1-\int_0^{L/2}Z_1\underline{\phi_{(0)}U''_{1(0)}}dZ_1\\ U_{3(0)}&=-\frac{1}{2}\int_0^Z U'^2_{1(0)}dZ_1-\frac{1}{2}\int_0^{L/2}U'^2_{1(0)}dZ_1.\end{aligned} \tag{4.21}$$

Similar to Eq. (3.21), the normality condition (or the existence condition for $\phi_{(1)}$ and $U_{1(1)}$) gives $\Delta P_{(0)}$. The underlined terms in Eq. (4.21) clearly show the importance of the 4th power of displacement in the potential energy: the displacement $U_{2(0)}$ would be zero if the 4th power of displacement were not accounted for.

4.3. Symmetric buckling mode

The symmetric buckling mode corresponds to an even function for $\phi_{(0)}$, and an odd function for $U_{1(0)}$. Without losing generality only half of the beam, $0\le Z\le L/2$, is considered. By introducing a new variable $\zeta=\sqrt{\overset{o}{P}/\sqrt{EI_2C}}Z$, integration of Eq. (4.20) and $\phi_{(0)}$ being an even function give

$$\frac{d^3\phi_{(0)}}{d\zeta^3}-\frac{2}{\zeta}\frac{d^2\phi_{(0)}}{d\zeta^2}+\zeta^2\frac{d\phi_{(0)}}{d\zeta}=0. \tag{4.22}$$

It is a 2nd order ODE for $d\phi_{(0)}/d\zeta$, and has the solution

$$\frac{d\phi_{(0)}}{d\zeta}=B_1\zeta^{3/2}J_{3/4}\left(\frac{\zeta^2}{2}\right) \tag{4.23}$$

for an even function $\phi_{(0)}$, where B_1 is a constant to be determined, J is the *Bessel* function of the first kind (Gradshteyn and Ryzhik, 2007). Integration of the above equation together with the boundary condition $\phi_{(0)}|_{Z=L/2}=0$ in Eq. (4.17) gives

$$\phi_{(0)}=-B_1\int_\zeta^{\zeta_{\max}}\zeta^{3/2}J_{3/4}\left(\frac{\zeta^2}{2}\right)d\zeta=B_1\left[\sqrt{\zeta_{\max}}J_{-1/4}\left(\frac{\zeta^2_{\max}}{2}\right)-\sqrt{\zeta}J_{-1/4}\left(\frac{\zeta^2}{2}\right)\right], \tag{4.24}$$

where $\zeta_{\max}=\sqrt{\overset{o}{P}/\sqrt{EI_2C}}(L/2)$ corresponds to the end $Z=L/2$. The parameter B_1 is determined from $\max(\phi_{(0)})=1$ as $B_1=\left[\sqrt{\zeta_{\max}}J_{\frac{-1}{4}}\left(\frac{\zeta^2_{\max}}{2}\right)-\frac{\sqrt{2}}{\Gamma(3/4)}\right]^{-1}$ in terms of the Γ function (Gradshteyn and Ryzhik, 2007), to ensure the parameter a in Eq. (4.15) to be the maximum angle of twist, $\phi_{\max}$.

Integration of the 1st equation in (4.17) gives $U_{1(0)}$ as

$$U_{1(0)}=L\frac{B_1}{2\zeta_{\max}}\sqrt{\frac{C}{EI_2}}\left[\sqrt{\zeta_{\max}}(\zeta_{\max}-\zeta)J_{3/4}\left(\frac{\zeta^2_{\max}}{2}\right)-\zeta\int_\zeta^{\zeta_{\max}}\frac{1}{\sqrt{\zeta}}J_{3/4}\left(\frac{\zeta^2}{2}\right)d\zeta\right]. \tag{4.25}$$

Its being an odd function requires $U_{1(0)}=0$ at $Z=0$, which gives

$$J_{3/4}\left(\frac{\zeta_{\max}^2}{2}\right)=0 \tag{4.26}$$

and has the solution $\zeta_{\max}=2.642$. The critical buckling load is then given by

$$\overset{\circ}{P}=27.93\frac{\sqrt{EI_2C}}{L^2}. \tag{4.27}$$

The constant $B_1=-0.5423$. Eqs. (4.24) and (4.25) can then be written explicitly as

$$\begin{aligned}\phi_{(0)}&=0.3742+0.5423\sqrt{\zeta}J_{\frac{1}{4}}\left(\frac{\zeta^2}{2}\right)\\ \frac{U_{1(0)}}{L}&=0.1026\sqrt{\frac{C}{EI_2}}\zeta\int_{\zeta}^{\zeta_{\max}}\frac{1}{\sqrt{\zeta}}J_{3/4}\left(\frac{\zeta^2}{2}\right)d\zeta=\sqrt{\frac{C}{EI_2}}\begin{bmatrix}0.07986\zeta-0.07879\zeta^3J_{-1/4}\left(\frac{\zeta^2}{2}\right)H_{-3/4}\left(\frac{\zeta^2}{2}\right)\\ +0.03051\zeta^3J_{3/4}\left(\frac{\zeta^2}{2}\right)s_{(-7/4),(1/4)}\left(\frac{\zeta^2}{2}\right)\end{bmatrix},\end{aligned} \tag{4.28}$$

where H is the Struve Function and s is the Lommel Function (Gradshteyn and Ryzhik, 2007). Eq. (4.21) then gives $U_{2(0)}$ and $U_{3(0)}$.

The applied nominal shear strain during postbuckling is obtained from Eqs. (4.21) and (4.28) as

$$\gamma_{applied}=\frac{U_2|_{Z=L/2}-U_2|_{Z=-L/2}}{L}=-\frac{2\phi_{\max}^2}{L}\int_0^{L/2}Z\underline{\phi_{(0)}U_{1(0)}''}dZ=\underline{0.2444\sqrt{\frac{C}{EI_2}}\phi_{\max}^2}. \tag{4.29}$$

It would give $\gamma_{applied}=0$ without the underlined terms, which clearly suggests the importance of higher-order terms in the curvature in the postbuckling analysis.

For a rectangular section with height $h \ll$ width b, $EI_1=Ehb^3/12$, $EI_2=Eh^3b/12$ and $C=Gh^3b/3$, where G is the shear modulus. The maximum bending strain, which is reached at the two ends of the beam, is the sum of bending strains at the onset of buckling and during postbuckling, and is given by

$$\varepsilon_{bending}=\frac{b}{2}\frac{\overset{\circ}{P}(L/2)}{EI_1}+\frac{h}{2}\max|U_1''|=\frac{h}{L}\left(7.474\sqrt{\gamma_{applied}\sqrt{\frac{G}{E}}}+13.97\frac{h}{b}\sqrt{\frac{G}{E}}\right)\approx 7.474\frac{h}{L}\sqrt{\gamma_{applied}\sqrt{\frac{G}{E}}}, \tag{4.30}$$

where the approximation on the 2nd line holds for $\phi_{\max}\gg h/b$. The maximum shear strain due to torsion is given by

$$\gamma_{torsion}=h\max|\phi'|=6.606\frac{h}{L}\sqrt{\gamma_{applied}\sqrt{\frac{E}{G}}}. \tag{4.31}$$

4.4. Anti-symmetric buckling mode

The anti-symmetric buckling mode corresponds to an odd function for $\phi_{(0)}$, and an even function for $U_{1(0)}$. Without losing generality only half of the beam, $0\le Z\le L/2$, is considered. Integration of Eq. (4.20) gives the same equation as (4.22) except that the right-hand side is replaced by a constant of integration B_2 (to be determined)

$$\frac{d^3\phi_{(0)}}{d\zeta^3}-\frac{2}{\zeta}\frac{d^2\phi_{(0)}}{d\zeta^2}+\zeta^2\frac{d\phi_{(0)}}{d\zeta}=B_2. \tag{4.32}$$

It has the solution

$$\frac{d\phi_{(0)}}{d\zeta}=B_2F(\zeta)+B_3\zeta^{3/2}J_{-3/4}\left(\frac{\zeta^2}{2}\right) \tag{4.33}$$

for an odd function $\phi_{(0)}$, where the constant B_3 is to be determined, and

$$F(\zeta)=-\frac{1}{3}\zeta^2+\frac{1}{4}\sqrt{\frac{2\pi}{\zeta}}\Gamma\left(\frac{3}{4}\right)\left[\zeta^2H_{5/4}\left(\frac{\zeta^2}{2}\right)-H_{1/4}\left(\frac{\zeta^2}{2}\right)\right]. \tag{4.34}$$

Its integration together with the boundary condition $\phi_{(0)}|_{Z=L/2}=0$ in Eq. (4.17) gives

$$\phi_{(0)}=-B_2\int_{\zeta}^{\zeta_{\max}}F(\zeta)d\zeta-B_3\left[\sqrt{\zeta_{\max}}J_{1/4}\left(\frac{\zeta_{\max}^2}{2}\right)-\sqrt{\zeta}J_{1/4}\left(\frac{\zeta^2}{2}\right)\right]. \tag{4.35}$$

Its being an odd function requires $\phi_{(0)}=0$ at $Z=0$, i.e.

$$B_2\int_0^{\zeta_{\max}} F(\zeta)d\zeta+B_3\sqrt{\zeta_{\max}}J_{1/4}\left(\frac{\zeta_{\max}^2}{2}\right)=0. \tag{4.36}$$

Integration of the 1st equation in (4.17) and the boundary condition $U'_{1(0)}\big|_{Z=L/2}=0$ give

$$\frac{d}{d\zeta}U_{1(0)}=-\frac{L}{2\zeta_{\max}}\sqrt{\frac{C}{EI_2}}\left\{B_2\int_\zeta^{\zeta_{\max}}\frac{1}{\zeta}\frac{dF(\zeta)}{d\zeta}d\zeta+B_3\int_\zeta^{\zeta_{\max}}\frac{1}{\zeta}\frac{d}{d\zeta}\left[\zeta^{\frac{3}{2}}J_{-3/4}\left(\frac{\zeta^2}{2}\right)\right]d\zeta\right\}. \tag{4.37}$$

It is an odd function (since $U_{1(0)}$ is even), which requires $U'_{1(0)}=0$ at $Z=0$. This gives

$$B_2\int_0^{\zeta_{\max}}\frac{1}{\zeta}\frac{dF(\zeta)}{d\zeta}d\zeta+B_3\int_0^{\zeta_{\max}}\frac{1}{\zeta}\frac{d}{d\zeta}\left[\zeta^{3/2}J_{-3/4}\left(\frac{\zeta^2}{2}\right)\right]d\zeta=0. \tag{4.38}$$

Eqs. (4.36) and (4.38) give two linear, homogeneous equations for B_2 and B_3. Their determinant must be zero in order to have a non-trivial solution, which gives the equation for the critical buckling load

$$\begin{vmatrix}\int_0^{\zeta_{\max}}F(\zeta)d\zeta & \sqrt{\zeta_{\max}}J_{1/4}\left(\frac{\zeta_{\max}^2}{2}\right)\\ \int_0^{\zeta_{\max}}\frac{1}{\zeta}\frac{dF(\zeta)}{d\zeta}d\zeta & \int_0^{\zeta_{\max}}\frac{1}{\zeta}\frac{d}{d\zeta}\left[\zeta^{3/2}J_{-3/4}\left(\frac{\zeta^2}{2}\right)\right]d\zeta\end{vmatrix}=0. \tag{4.39}$$

It has the solution $\zeta_{\max}=3.038$. The critical buckling load is then given by

$$\overset{\circ}{P}=36.92\frac{\sqrt{EI_2C}}{L^2}, \tag{4.40}$$

which is larger than Eq. (4.27) for the symmetric mode.

Integration of Eq. (4.37) and the boundary condition $U_{1(0)}|_{Z=L/2}=0$ give

$$U_{1(0)}=\frac{L}{2\zeta_{\max}}\sqrt{\frac{C}{EI_2}}\left\{\begin{array}{l}B_2\left[\frac{\zeta_{\max}-\zeta}{\zeta_{\max}}F(\zeta_{\max})-\zeta\int_\zeta^{\zeta_{\max}}\frac{F(\zeta)}{\zeta^2}d\zeta\right]\\ +B_3\left[\sqrt{\zeta_{\max}}(\zeta_{\max}-\zeta)J_{-3/4}\left(\frac{\zeta_{\max}^2}{2}\right)-\zeta\int_\zeta^{\zeta_{\max}}\frac{1}{\sqrt{\zeta}}J_{-3/4}\left(\frac{\zeta^2}{2}\right)d\zeta\right]\end{array}\right\}. \tag{4.41}$$

The parameter a in Eq. (4.15) is the ratio of maximum displacement to L, i.e., $a=U_{1\max}/L$, which, together with Eq. (4.41), give

$$B_2F(\zeta_{\max})+B_3\left[\zeta_{\max}^{3/2}J_{-3/4}\left(\frac{\zeta_{\max}^2}{2}\right)-\frac{2}{\pi}\Gamma\left(\frac{3}{4}\right)\right]=2\zeta_{\max}\sqrt{\frac{EI_2}{C}}. \tag{4.42}$$

Eqs. (4.36) and (4.42) determine $B_2=3.850\sqrt{EI_2/C}$ and $B_3=-1.166\sqrt{EI_2/C}$. Eqs. (4.35) and (4.41) can then be written explicitly as

$$\begin{aligned}\phi_{(0)}&=-\sqrt{\frac{EI_2}{C}}\left[0.7250+3.850\int_\zeta^{3.038}F(\zeta)d\zeta+1.166\sqrt{\zeta}J_{1/4}\left(\frac{\zeta^2}{2}\right)\right]\\ \frac{U_{1(0)}}{L}&=0.8503-0.2799\zeta-0.6337\zeta\int_\zeta^{3.038}\frac{F(\zeta)}{\zeta^2}d\zeta+0.1919\zeta\int_\zeta^{3.038}\frac{1}{\sqrt{\zeta}}J_{-3/4}\left(\frac{\zeta^2}{2}\right)d\zeta.\end{aligned} \tag{4.43}$$

Eq. (4.21) then gives $U_{2(0)}$ and $U_{3(0)}$.

The applied nominal shear strain during postbuckling is obtained from Eqs. (4.21) and (4.43) as

$$\gamma_{applied}=\frac{U_2|_{Z=L/2}-U_2|_{Z=-L/2}}{L}=-\frac{2U_{1\max}^2}{L^3}\int_0^{L/2}Z\underline{\phi_{(0)}U''_{1(0)}}dZ=\underline{10.38\sqrt{\frac{EI_2}{C}}\left(\frac{U_{1\max}}{L}\right)^2}. \tag{4.44}$$

It would also give $\gamma_{applied}=0$ without the underlined terms, which confirms the importance of higher-order terms in the curvature in the postbuckling analysis.

The maximum bending strain at the onset of buckling is $\varepsilon_{bending}=18.46\left[h^2/(Lb)\right]\sqrt{G/E}$. The maximum bending strain and torsion (shear) strain due to postbuckling are

$$\varepsilon_{bending}=6.833\frac{h}{L}\sqrt{\gamma_{applied}\sqrt{\frac{G}{E}}}, \tag{4.45}$$

$$\gamma_{torsion}=h\max|\phi'|=8.632\frac{h}{L}\sqrt{\gamma_{applied}\sqrt{\frac{E}{G}}}. \tag{4.46}$$

Their comparison with Eqs. (4.30) and (4.31) suggests that the anti-symmetric buckling mode gives a smaller bending strain but a larger shear strain than the symmetric buckling mode.

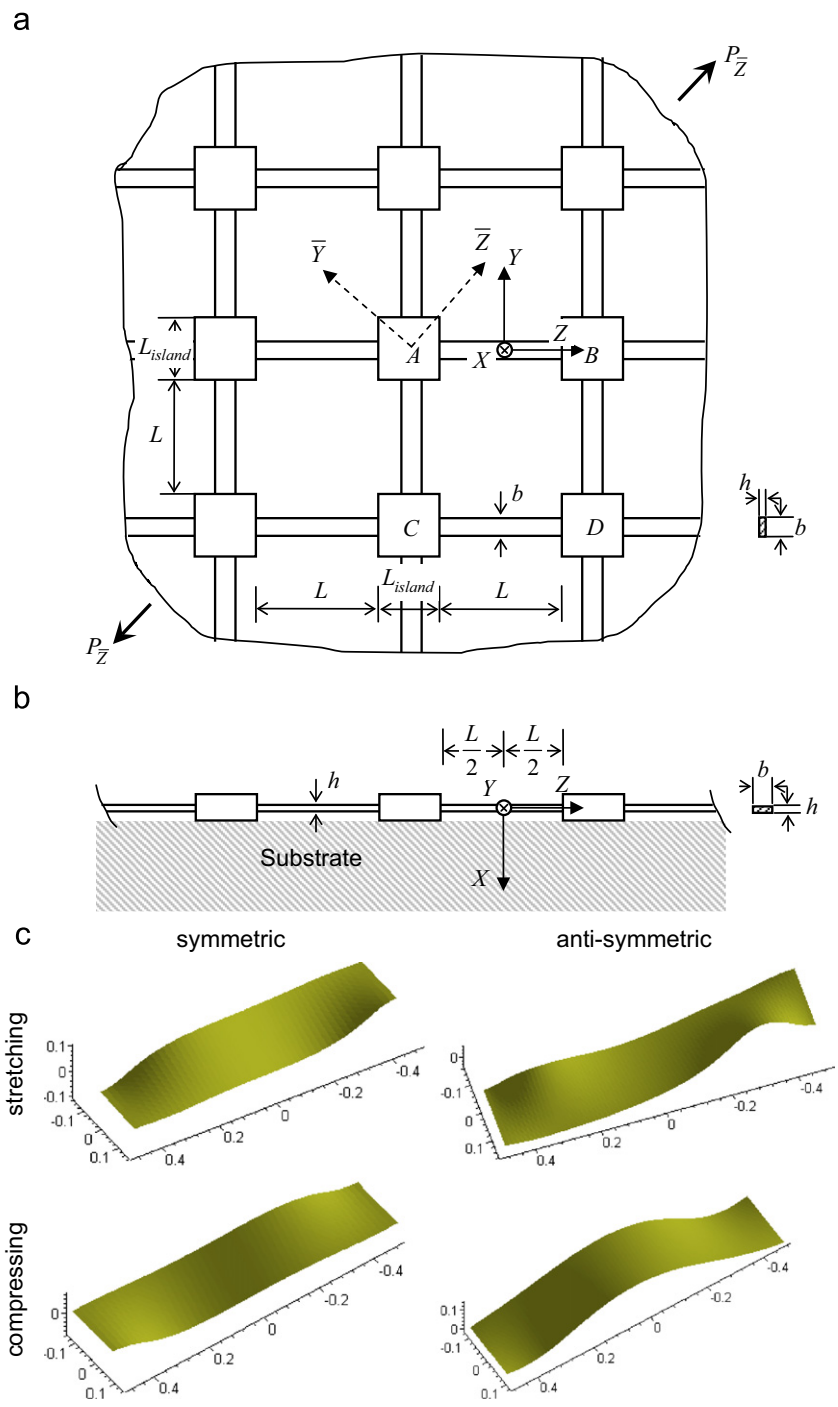

Fig. 4. Illustration of the island-bridge, mesh structure in the stretchable electronics subject to stretching/compressing along the 45° (diagonal) direction; (a) top view; (b) side view; and (c) the symmetric and anti-symmetric buckling modes for both stretching and compressing.

Fig. 3c shows the symmetric and anti-symmetric buckling modes in Sections 4.3 and 4.4, respectively. The applied nominal shear strain is $\gamma_{applied}=20\%$, and $C/(EI_2)=1.57$. The buckling mode for the anti-symmetric appears to be rather similar to the experimentally observed buckling profile in Fig. 1b for the shear case.

The analysis in this section also holds for the island-bridge, mesh structure in stretchable electronics (Fig. 4) subject to pure shear. For example, the bending and torsion strains in Eqs. (4.30), (4.31), (4.45) and (4.46) still hold if the applied nominal shear strain $\gamma_{applied}$ to the beam is replaced by $\gamma(L+L_{island})/L$, where γ is the shear strain applied to the island-bridge, mesh structure, and L_{island} is the island size (Fig. 4).

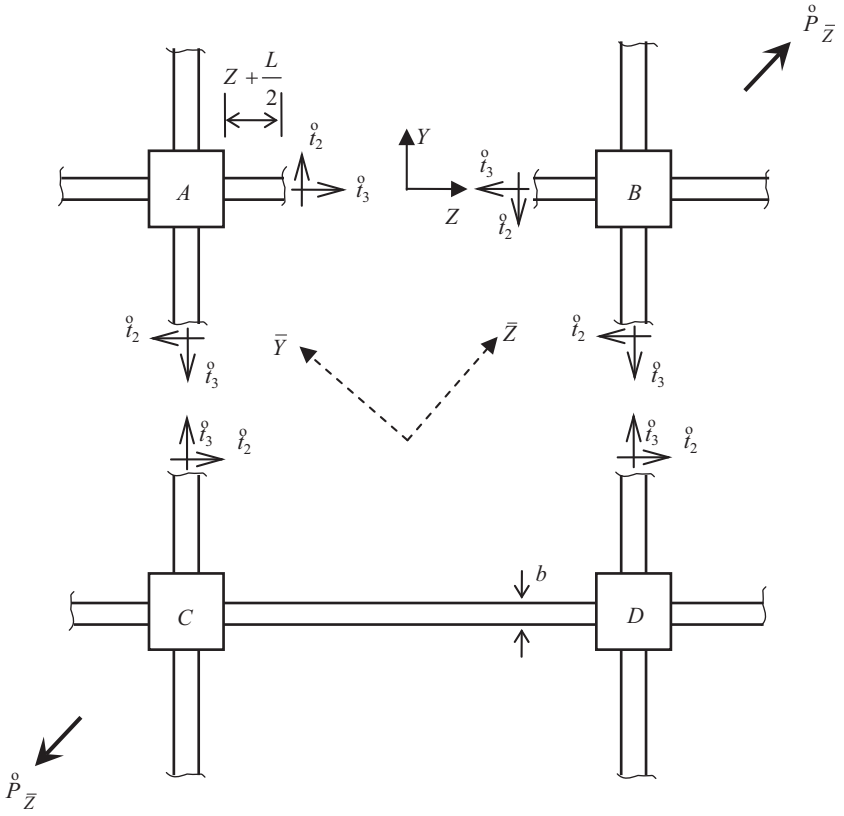

Fig. 5. Free-body diagram of the island-bridge, mesh structure prior to the onset of buckling.

5. Buckling of island-bridge, mesh structure in stretchable electronics

Fig. 4a shows the top view of an island-bridge, mesh structure in stretchable electronics (Kim et al., 2008b). The square islands of size L_{island} are linked by bridges of length L. The islands are well attached to the substrate, but bridges are not, as seen from the side view in Fig. 4b. The bridges buckle to shield the islands from large deformation. Let Z denote the central axis of the bridge before deformation, with $Z=0$ at the bridge center (Fig. 4a), and Y axis in the plane of the island-bridge, mesh structure and be normal to Z.

Euler buckling occurs in bridges for the island-bridge, mesh structure subject to compression along Z or Y directions. Tension or compression along the diagonal direction ($\bar{Z}$ in Fig. 4a) of the square islands, as in experiments, is studied in the following.

5.1. State prior to the onset of buckling

Let $P_{\bar{Z}}$ denote the tension force (per unit length) along $\bar{Z}$ direction (Fig. 4a). There are no distributed force and moment, $\boldsymbol{p}=\boldsymbol{q}=0$. The force, bending moment and torque in bridges $\overset{o}{t}_1=\overset{o}{m}_2=\overset{o}{m}_3=0$, and the non-zero forces and bending moment $\overset{o}{t}_2$, $\overset{o}{t}_3$ and $\overset{o}{m}_1$ are symmetric about $\bar{Z}$ and $\bar{Y}$ directions.

Fig. 5 shows the free body diagram of the left and lower half of the island-bridge, mesh structure that is cut along $\bar{Y}$ direction. The forces $\overset{o}{t}_2$ and $\overset{o}{t}_3$ in the bridges along Z and Y directions satisfy the symmetry about $\bar{Z}$ and $\bar{Y}$ directions. Equilibrium of forces in $\bar{Z}$ direction gives $\overset{o}{t}_2+\overset{o}{t}_3-\overset{o}{P}_{\bar{Z}}(L+L_{island})=0$. Similarly, force equilibrium in $\bar{Y}$ direction gives $\overset{o}{t}_2-\overset{o}{t}_3=0$. These give

$$\overset{o}{t}_2=\frac{1}{2}\overset{o}{P}_{\bar{Z}}(L+L_{island}),\quad \overset{o}{t}_3=\frac{1}{2}\overset{o}{P}_{\bar{Z}}(L+L_{island}). \tag{5.1}$$

The islands do not rotate due to symmetry about $\bar{Z}$ and $\bar{Y}$ directions. The bending moment $\overset{o}{m}_1$ can then be found as

$$\overset{o}{m}_1=\frac{1}{2}\overset{o}{P}_{\bar{Z}}(L+L_{island})Z \quad \text{for} \quad -\frac{L}{2}\le Z\le\frac{L}{2}. \tag{5.2}$$

5.2. Equations for postbuckling analysis

Let $\overset{\circ}{P}_{\bar{Z}}$ denote the critical tension at the onset of buckling, and $\Delta P_{\bar{Z}}$ the changes during postbuckling. Only the displacements along Z and Y directions are not zero prior to the onset of buckling. Therefore the orders of displacements and rotation ϕ during postbuckling are the same as Eq. (4.2). The stretch and curvatures are still given by Eqs. (4.3) and (4.4). Their substitution into Eqs. (2.11)–(2.13) gives the ODEs for $\boldsymbol{U}$ and ϕ

$$C\phi''+(EI_1-EI_2)U_1''(U_2''-\underline{\phi U_1''})-\overset{\circ}{m}_1\left[U_1''+\underline{\phi U_2''-(U_1'U_3')'-\frac{1}{2}\phi^2U_1''-\frac{1}{3}(U_1'^3)'}\right]+O\left[(U_1)^5\right]=0, \tag{5.3}$$

$$\begin{aligned}&EI_2\left\{U_1^{(4)}-U_1'''\left(U_3'+\frac{1}{2}U_1'^2\right)'-\phi'^2U_1''+\left[\underline{\phi U_2''-(U_1'U_3')'-\frac{1}{2}\phi^2U_1''-\frac{1}{3}(U_1'^3)'}\right]''\right\}\\&\quad-EI_1\left[\phi''(U_2''-\underline{\phi U_1''})+2\phi'(U_2''-\underline{\phi U_1''})'\right]+C\left[\phi''(U_2''-\underline{\phi U_1''})+\phi'(U_2''-\underline{\phi U_1''})'+\phi'^2U_1''\right]-EAU_1''\left(U_3'+\frac{1}{2}U_1'^2\right)+\overset{\circ}{t}_2\phi'\\&-\overset{\circ}{t}_3\left[U_1''\left(1+U_3'+\frac{1}{2}U_1'^2\right)+\underline{\phi U_2''-(U_1'U_3')'-\frac{1}{2}\phi^2U_1''-\frac{1}{3}(U_1'^3)'}\right]+(\overset{\circ}{m}_1\phi')'-\overset{\circ}{m}_1\phi'\left(U_3'+\frac{1}{2}U_1'^2\right)'+O\left[(U_1)^5\right]=0,\end{aligned} \tag{5.4}$$

$$EI_1(U_2''-\underline{\phi U_1''})''+EI_2(\phi''U_1''+2\phi'U_1''')-C(\phi'U_1'')'+\overset{\circ}{t}_2\left(U_3'+\frac{1}{2}U_1'^2\right)'-\overset{\circ}{t}_3(U_2''-\underline{\phi U_1''})+\overset{\circ}{m}_1\phi'^2+O\left[(U_1)^4\right]=0, \tag{5.5}$$

$$\left[EA\left(U_3'+\frac{1}{2}U_1'^2\right)+\frac{1}{2}EI_2U_1''^2\right]'-\overset{\circ}{t}_2(U_2''-\underline{\phi U_1''})+\overset{\circ}{m}_1\phi'U_1''+O\left[(U_1)^4\right]=0, \tag{5.6}$$

where the underlined are the higher-order terms in the curvatures neglected in the existing postbuckling analysis (von Karman and Tsien, 1941; Budiansky, 1973). The increments of axial force Δt_3 and bending moment and torque $\Delta\boldsymbol{m}$ can be obtained from Eqs. (2.13), (4.3) and (4.4). The shear forces are given by

$$\begin{aligned}\lambda\Delta t_1&=-EI_2\left[U_1''+\underline{\phi U_2''-(U_1'U_3')'-\frac{1}{2}\phi^2U_1''-\frac{1}{3}(U_1'^3)'}\right]'+(EI_1-C)\phi'(U_2''-\underline{\phi U_1''})-\overset{\circ}{m}_1\phi'+O\left[(U_1)^5\right]\\\lambda\Delta t_2&=-EI_1(U_2''-\underline{\phi U_1''})'-(EI_2-C)\phi'U_1''-\overset{\circ}{t}_2\left(U_3'+\frac{1}{2}U_1'^2\right)+O\left[(U_1)^4\right]\end{aligned} \tag{5.7}$$

Eqs. (5.3)–(5.7) hold for arbitrary equilibrium state $\overset{\circ}{\boldsymbol{t}}$ and $\overset{\circ}{\boldsymbol{m}}$ prior to the onset of buckling. For example, for the state in Eq. (4.1), the above equations degenerate to Eqs. (4.5)–(4.9).

The displacements U_2 and U_3 at the midpoint are zero to remove the rigid body translation

$$U_2=U_3=0 \quad \text{at} \quad Z=0 \tag{5.8}$$

The other boundary conditions (4.11) and (4.12) still hold. The traction conditions at the end $Z=L/2$ are $\Delta t_2=\Delta t_3=\Delta P_{\bar{Z}}(L+L_{island})/2$, which can be expressed in terms of the displacements as

$$\begin{aligned}&U_3'-\frac{\Delta P_{\bar{Z}}(L+L_{island})}{2EA}+O\left[(U_1)^4\right]=0\\&(U_2''-\underline{\phi U_1''})'+\frac{EI_2-C}{EI_1}\phi'U_1''+\frac{\overset{\circ}{t}_2}{EI_1}U_3'+\frac{\Delta P_{\bar{Z}}(L+L_{island})}{2EI_1}+O\left[(U_1)^4\right]=0 \quad \text{at} \quad Z=L/2.\end{aligned} \tag{5.9}$$

5.3. Perturbation method

The perturbation method is used to solve the ODEs (5.3)–(5.6) with boundary conditions (4.11), (4.12), (5.8), and (5.9). Let a denote the ratio of the maximum deflection $U_{1\max}$ to the beam length L or the maximum twist $\phi_{\max}$. The displacements and rotation are expanded to the power series of a as in Eq. (4.15). Similarly, $\Delta P_{\bar{Z}}$ is written as

$$\Delta P_{\bar{Z}}=a^2\Delta P_{\bar{Z}(0)}+\ldots. \tag{5.10}$$

Substitution of Eqs. (4.15) and (5.10) into Eqs. (5.3)–(5.6), (5.8) and (5.9) gives

$$\begin{cases}C\phi_{(0)}''-\overset{\circ}{m}_1U_{1(0)}''=0\\EI_2U_{1(0)}^{(4)}+\overset{\circ}{t}_2\phi_{(0)}'-\overset{\circ}{t}_3U_{1(0)}''+(\overset{\circ}{m}_1\phi_{(0)}')'=0\\\phi_{(0)}\big|_{Z=\pm L/2}=U_{1(0)}\big|_{Z=\pm L/2}=U_{1(0)}'|_{Z=\pm L/2}=0,\end{cases} \tag{5.11}$$

$$\begin{cases} EI_1(U''_{2(0)}-\underline{\phi_{(0)}U''_{1(0)}})''+EI_2(\phi''_{(0)}U''_{1(0)}+2\phi'_{(0)}U'''_{1(0)})-C(\phi'_{(0)}U''_{1(0)})' \\ +\overset{o}{t}_2\left(U'_{3(0)}+\frac{1}{2}U'^2_{1(0)}\right)'-\overset{o}{t}_3(U''_{2(0)}-\underline{\phi_{(0)}U''_{1(0)}})+\overset{o}{m}_1\phi'^2_{(0)}=0 \\ \left[EA\left(U'_{3(0)}+\frac{1}{2}U'^2_{1(0)}\right)+\frac{1}{2}EI_2U''^2_{1(0)}\right]'-\overset{o}{t}_2(U''_{2(0)}-\underline{\phi_{(0)}U''_{1(0)}})+\overset{o}{m}_1\phi'_{(0)}U''_{1(0)}=0 \\ U_{2(0)}|_{Z=0}=U_{3(0)}|_{Z=0}=U'_{2(0)}|_{Z=\pm L/2}=U'_{3(0)}|_{Z=L/2}-\frac{\Delta P_{\overline{Z}(0)}(L+L_{island})}{2EA}=0 \\ \left[(U''_{2(0)}-\underline{\phi_{(0)}U''_{1(0)}})'+\frac{EI_2-C}{EI_1}\phi'_{(0)}U''_{1(0)}+\frac{1}{EI_1}\overset{o}{t}_2U'_{3(0)}\right]_{Z=L/2}=-\frac{\Delta P_{\overline{Z}(0)}(L+L_{island})}{2EI_1} \end{cases} \tag{5.12}$$

for the leading powers of a, and

$$\begin{cases} C\phi''_{(1)}-\overset{o}{m}_1U''_{1(1)}=-(EI_1-EI_2)U''_{1(0)}(U''_{2(0)}-\underline{\phi_{(0)}U''_{1(0)}})+\overset{o}{m}_1\left[\underline{\phi_{(0)}U''_{2(0)}-(U'_{1(0)}U'_{3(0)})'-\frac{1}{2}\phi^2_{(0)}U''_{1(0)}-\frac{1}{3}(U'^3_{1(0)})'}\right] \\ EI_2U^{(4)}_{1(1)}+\overset{o}{t}_2\phi'_{(1)}-\overset{o}{t}_3U''_{1(1)}+(\overset{o}{m}_1\phi'_{(1)})' \\ =EI_2\left\{U'''_{1(0)}\left(U'_{3(0)}+\frac{1}{2}U'^2_{1(0)}\right)'+\phi'^2_{(0)}U''_{1(0)}-\left[\underline{\phi_{(0)}U''_{2(0)}-(U'_{1(0)}U'_{3(0)})'-\frac{1}{2}\phi^2_{(0)}U''_{1(0)}-\frac{1}{3}(U'^3_{1(0)})'}\right]''\right\} \\ \quad+EI_1\left[\phi''_{(0)}(U''_{2(0)}-\underline{\phi_{(0)}U''_{1(0)}})+2\phi'_{(0)}(U''_{2(0)}-\underline{\phi_{(0)}U''_{1(0)}})'\right]-C\left[\phi''_{(0)}(U''_{2(0)}-\underline{\phi_{(0)}U''_{1(0)}})+\phi'_{(0)}(U''_{2(0)}-\underline{\phi_{(0)}U''_{1(0)}})'+\phi'^2_{(0)}U''_{1(0)}\right] \\ \quad+EAU''_{1(0)}\left(U'_{3(0)}+\frac{1}{2}U'^2_{1(0)}\right)+\overset{o}{t}_3\left[U''_{1(0)}\left(U'_{3(0)}+\frac{1}{2}U'^2_{1(0)}\right)+\underline{\phi_{(0)}U''_{2(0)}-(U'_{1(0)}U'_{3(0)})'-\frac{1}{2}\phi^2_{(0)}U''_{1(0)}-\frac{1}{3}(U'^3_{1(0)})'}\right] \\ \quad+\overset{o}{m}_1\phi'_{(0)}\left(U'_{3(0)}+\frac{1}{2}U'^2_{1(0)}\right)' \\ [\phi_{(1)}+\psi^{(2)}_{(0)}+\psi^{(3)}_{(0)}]|_{Z=\pm L/2}=U_{1(1)}|_{Z=\pm L/2}=U'_{1(1)}\Big|_{Z=\pm L/2}=0 \end{cases} \tag{5.13}$$

for the next power of a, where

$$\psi^{(2)}_{(0)}=\frac{1}{2}\int_0^Z(U'_{1(0)}U''_{2(0)}-U''_{1(0)}U'_{2(0)})dZ \quad \text{and} \quad \psi^{(3)}_{(0)}=-\frac{1}{4}\phi_{(0)}\left(\frac{2}{3}\phi^2_{(0)}+U'^2_{1(0)}\right).$$

Elimination of $U_{1(0)}$ in Eq. (5.11) yields the equation for $\phi_{(0)}$

$$\frac{d}{dZ}\left\{\phi'''_{(0)}-\frac{2}{Z}\phi''_{(0)}+\frac{[\overset{o}{P}_{\overline{Z}}(L+L_{island})Z]^2}{4EI_2C}\phi'_{(0)}-\frac{\overset{o}{P}_{\overline{Z}}(L+L_{island})}{2EI_2}\phi'_{(0)}\right\}=0 \tag{5.14}$$

for the state prior to the onset of buckling in Eqs. (5.1) and (5.2). The symmetric and anti-symmetric buckling modes correspond to even and odd $\phi_{(0)}$, respectively, and $U_{1(0)}$ is odd for an even $\phi_{(0)}$, and is even for an odd $\phi_{(0)}$.

For bridges with a narrow cross section such that $EI_1 \gg EI_2, C$ as in experiments, Eq. (5.12) can be significantly simplified by neglecting $EI_2/(EI_1)$ and $C/(EI_1)$

$$\begin{cases} (U''_{2(0)}-\underline{\phi_{(0)}U''_{1(0)}})''=0 \\ U_{2(0)}|_{Z=0}=U'_{2(0)}\Big|_{Z=\pm L/2}=(U''_{2(0)}-\underline{\phi_{(0)}U''_{1(0)}})'\Big|_{Z=L/2}=0 \end{cases}, \quad \begin{cases} \left(U'_{3(0)}+\frac{1}{2}U'^2_{1(0)}\right)'=0 \\ U_{3(0)}|_{Z=0}=U'_{3(0)}\Big|_{Z=L/2}=0 \end{cases}, \tag{5.12a}$$

where the deformation at the onset of buckling is negligible since $\overset{o}{P}_{\overline{Z}}$ and $\Delta P_{\overline{Z}(0)}$ are proportional to $\sqrt{EI_2C}$ (to be shown in Sections 5.4 and 5.5) and the bridge length L is much larger than the cross section dimension (e.g., thickness). The above equation, together with $\phi_{(0)}$ and $U_{1(0)}$ being opposite even or odd functions, give $U''_{2(0)}=\underline{\phi_{(0)}U''_{1(0)}}$ and $U'_{3(0)}=-U'^2_{1(0)}/2$. Its solution is

$$U_{2(0)}=-Z\int_Z^{L/2}\underline{\phi_{(0)}U''_{1(0)}}dZ_1-\int_0^Z Z_1\underline{\phi_{(0)}U''_{1(0)}}dZ_1$$

$$U_{3(0)}=-\frac{1}{2}\int_0^Z U'^2_{1(0)}dZ_1. \tag{5.15}$$

For both symmetric or anti-symmetric buckling modes, $U_{2(0)}$ and $U_{3(0)}$ are always odd functions. Similar to Eq. (3.21), the normality condition for Eq. (5.13) gives $\Delta P_{\overline{Z}(0)}$. The displacement $U_{2(0)}$ would be zero in Eq. (5.15) without accounting for the 4th power of displacement in the potential energy.

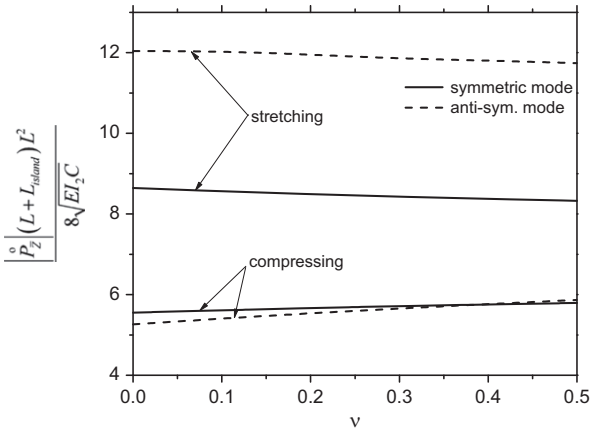

Fig. 6. The normalized critical buckling load versus the Poisson's ratio of the bridge for the symmetric and anti-symmetric buckling modes, subject to stretching or compressing along 45° (diagonal) direction.

5.4. Symmetric buckling mode

For an even function $\phi_{(0)}$ and odd function $U_{1(0)}$, only half of the beam, $0 \le Z \le L/2$, is considered. Integration of Eq. (5.14) and $\phi_{(0)}$ being an even function give

$$\frac{d^3\phi_{(0)}}{d\zeta^3} - \frac{2}{\zeta}\frac{d^2\phi_{(0)}}{d\zeta^2} + \zeta^2\frac{d\phi_{(0)}}{d\zeta} - \alpha\frac{d\phi_{(0)}}{d\zeta} = 0, \tag{5.16}$$

where $\zeta = \sqrt{\left|\overset{\circ}{P}_{\bar{Z}}\right|(L+L_{island})/(2\sqrt{EI_2C})}Z$, $\alpha = \sqrt{C/(EI_2)}\,\mathrm{sign}(\overset{\circ}{P}_{\bar{Z}})$, $\mathrm{sign}(\overset{\circ}{P}_{\bar{Z}}) = 1$ for tension and $\mathrm{sign}(\overset{\circ}{P}_{\bar{Z}}) = -1$ for compression. The solution of the above equation is

$$\frac{d\phi_{(0)}}{d\zeta} = B_4\sqrt{\zeta}\,\mathrm{Re}\left[M_{i(\alpha/4),(3/4)}(i\zeta^2)\right] \tag{5.17}$$

for an even function $\phi_{(0)}$, where B_4 is a constant to be determined, Re stands for the real part, M is the *Whittaker M* function with indices $i\alpha/4$ and 3/4 (Gradshteyn and Ryzhik, 2007), and $i = \sqrt{-1}$. Integration of Eq. (5.17) together with the boundary condition $\phi_{(0)}|_{Z=L/2} = 0$ in Eq. (5.11) gives

$$\phi_{(0)} = -B_4\int_{\zeta}^{\zeta_{\max}} \sqrt{\zeta}\,\mathrm{Re}[M_{i(\alpha/4),(3/4)}(i\zeta^2)]d\zeta, \tag{5.18}$$

where $\zeta_{\max} = \sqrt{\left|\overset{\circ}{P}_{\bar{Z}}\right|(L+L_{island})L^2/(8\sqrt{EI_2C})}$ corresponds to the end $Z=L/2$. The parameter B_4 is determined from $\max(\phi_{(0)}) = 1$ as $B_4 = -\left\{\int_0^{\zeta_{\max}} \sqrt{\zeta}\,\mathrm{Re}[M_{i(\alpha/4),(3/4)}(i\zeta^2)]d\zeta\right\}^{-1}$, which ensures the parameter a in Eq. (4.15) to be the maximum angle of twist, ϕ_{max}.

Integration of the 1st equation in (5.11) gives $U_{1(0)}$ as

$$U_{1(0)} = -L\frac{\alpha B_4}{2\zeta_{\max}}\left\{\zeta\int_{\zeta}^{\zeta_{\max}}\frac{1}{\zeta^{3/2}}\mathrm{Re}\left[M_{i(\alpha/4),(3/4)}(i\zeta^2)\right]d\zeta - \frac{\zeta_{\max}-\zeta}{\sqrt{\zeta_{\max}}}\mathrm{Re}\left[M_{i(\alpha/4),(3/4)}(i\zeta_{\max}^2)\right]\right\}. \tag{5.19}$$

Its being an odd function requires $U_{1(0)}=0$ at $Z=0$, which gives the following simple equation for the critical buckling load:

$$\mathrm{Re}[M_{i(\alpha/4),(3/4)}(i\zeta_{\max}^2)] = 0, \tag{5.20}$$

which has the solution $\zeta_{\max} = \zeta_{\max}(\alpha)$. The critical buckling load is

$$\left|\overset{\circ}{P}_{\bar{Z}}\right| = \frac{8\sqrt{EI_2C}}{(L+L_{island})L^2}[\zeta_{\max}(\alpha)]^2. \tag{5.21}$$

The normalized critical buckling load, $\left|\overset{\circ}{P}_{\bar{Z}}\right|(L+L_{island})L^2/(8\sqrt{EI_2C})$, is shown versus the Poisson's ratio v of the bridge in Fig. 6, where $\alpha = \sqrt{2/(1+v)}\,\mathrm{sign}(\overset{\circ}{P}_{\bar{Z}})$ for a rectangular cross section of the bridge. The critical buckling load for stretching is clearly larger than that for compressing, and both are essentially independent of v.

Table 1
The coefficients β versus the Poisson's ratio v of the bridge for the symmetric and anti-symmetric buckling modes under 45° stretching.

Poisson's ratio	Stretching					
	Symmetric			Anti-symmetric		
	$\mathring{\beta}^{sym}_{bending}$	$\beta^{sym}_{bending}$	$\beta^{sym}_{torsion}$	$\mathring{\beta}^{anti}_{bending}$	$\beta^{anti}_{bending}$	$\beta^{anti}_{torsion}$
$v=0.1$	11.55	6.796	10.07	16.23	8.111	12.75
$v=0.2$	10.96	6.622	10.20	15.43	7.775	12.94
$v=0.3$	10.46	6.467	10.33	14.71	7.671	13.11
$v=0.4$	10.01	6.328	10.45	14.11	7.262	13.29
$v=0.5$	9.614	6.201	10.56	13.56	6.897	13.46

Table 2
The coefficients β versus the Poisson's ratio v of the bridge for the symmetric and anti-symmetric buckling modes under 45° compressing.

Poisson's ratio	Compressing					
	Symmetric			Anti-symmetric		
	$\mathring{\beta}^{sym}_{bending}$	$\beta^{sym}_{bending}$	$\beta^{sym}_{torsion}$	$\mathring{\beta}^{anti}_{bending}$	$\beta^{anti}_{bending}$	$\beta^{anti}_{torsion}$
$v=0.1$	7.570	5.503	6.216	7.290	4.639	7.328
$v=0.2$	7.316	5.410	6.426	7.149	4.557	7.680
$v=0.3$	7.087	5.324	6.623	7.016	4.481	8.008
$v=0.4$	6.880	5.246	6.807	6.891	4.409	8.313
$v=0.5$	6.691	5.173	6.981	6.773	4.342	8.600

Eq. (5.19) can then be simplified to

$$\frac{U_{1(0)}}{L} = -B_4 \frac{\alpha\zeta}{2\zeta_{\max}} \int_{\zeta}^{\zeta_{\max}} \frac{1}{\zeta^{3/2}} \mathrm{Re}\left[M_{i(\alpha/4),(3/4)}(i\zeta^2)\right] d\zeta. \tag{5.22}$$

Eq. (5.15) then gives $U_{2(0)}$ and $U_{3(0)}$.

The applied strain along $\overline{Z}$ (45°) direction during postbuckling is

$$\varepsilon_{45^\circ} = \frac{1}{L+L_{island}} \left(\int_{-L/2}^{L/2} U_3' dZ + \int_{-L/2}^{L/2} U_2' dZ \right) = \frac{L\phi_{\max}^2}{L+L_{island}} \left\{ \frac{\alpha}{\zeta_{\max}} \int_0^{\zeta_{\max}} \underline{\left(\frac{d\phi_{(0)}}{d\zeta}\right)^2} d\zeta - 2\zeta_{\max} \int_0^{\zeta_{\max}} \left[\frac{d}{d\zeta}\left(\frac{U_{1(0)}}{L}\right)\right]^2 d\zeta \right\}, \tag{5.23}$$

where the coefficient inside (von Karman and Tsien, 1941) depends only on α since $\zeta_{\max} = \zeta_{\max}(\alpha)$.

For a rectangular section with height $h \ll$ width b, $EI_1 = Ehb^3/12$, $EI_2 = Eh^3b/12$ and $C = Gh^3b/3$. The maximum bending strain is the sum of bending strains at the onset of buckling and during postbuckling, and is given by

$$\varepsilon_{bending} = \frac{h}{L} \left(\beta^{sym}_{bending} \sqrt{\frac{L+L_{island}}{L} |\varepsilon_{45^\circ}|} + \mathring{\beta}^{sym}_{bending} \frac{h}{b} \right). \tag{5.24}$$

The maximum shear strain due to torsion is given by

$$\gamma_{torsion} = \beta^{sym}_{torsion} \frac{h}{L} \sqrt{\frac{L+L_{island}}{L} |\varepsilon_{45^\circ}|}. \tag{5.25}$$

The coefficients β's in the above two equations are shown versus the Poisson's ratio v of the bridge in Tables 1 and 2 for stretching and compressing along 45°, respectively. They are essentially independent of v.

Without accounting for the 4th power of displacement in the potential energy one could not study postbuckling for stretching along 45° because Eq. (5.23) would give a compressive strain $\varepsilon_{45^\circ} < 0$. For compressing along 45°, the maximum bending and shear strains would be overestimated by more than a factor of 2.

5.5. Anti-symmetric buckling mode

For an odd function $\phi_{(0)}$ and even function $U_{1(0)}$, only half of the beam, $0 \le Z \le L/2$, is considered. Integration of Eq. (5.14) and $\phi_{(0)}$ being an odd function give

$$\frac{d^3\phi_{(0)}}{d\zeta^3} - \frac{2}{\zeta}\frac{d^2\phi_{(0)}}{d\zeta^2} + \zeta^2 \frac{d\phi_{(0)}}{d\zeta} - \alpha \frac{d\phi_{(0)}}{d\zeta} = B_5, \tag{5.26}$$

where B_5 is a constant of integration to be determined. The solution of the above equation is

$$\frac{d\phi_{(0)}}{d\zeta} = B_5 D(\zeta) + B_6 \sqrt{\zeta}\,\mathrm{Re}\left[M_{i(\alpha/4),(-3/4)}(i\zeta^2)\right] \tag{5.27}$$

for an odd function $\phi_{(0)}$, where B_5 and B_6 are constants to be determined, the function D is given in Appendix A, M is the *Whittaker M* function with indices $i\alpha/4$ and $-3/4$ (Gradshteyn and Ryzhik, 2007). Integration of Eq. (5.27) together with the boundary condition $\phi_{(0)}|_{Z=L/2}=0$ in Eq. (5.11) gives

$$\phi_{(0)} = -B_5 \int_{\zeta}^{\zeta_{\max}} D(\zeta)d\zeta - B_6 \int_{\zeta}^{\zeta_{\max}} \sqrt{\zeta}\,\mathrm{Re}[M_{i(\alpha/4),(-3/4)}(i\zeta^2)]d\zeta. \tag{5.28}$$

Its being an odd function requires $\phi_{(0)}=0$ at $Z=0$, i.e.

$$B_5 \int_{0}^{\zeta_{\max}} D(\zeta)d\zeta + B_6 \int_{0}^{\zeta_{\max}} \sqrt{\zeta}\,\mathrm{Re}[M_{i(\alpha/4),(-3/4)}(i\zeta^2)]d\zeta = 0. \tag{5.29}$$

Integration of the 1st equation in (5.11) and the boundary condition $U'_{1(0)}\Big|_{Z=L/2}=0$ give

$$\frac{d}{d\bar{\zeta}}U_{1(0)} = -L\frac{\alpha}{2\zeta_{\max}}\left\langle B_5 \int_{\zeta}^{\zeta_{\max}} \frac{1}{\zeta}\frac{dD(\zeta)}{d\zeta}d\zeta + B_6 \int_{\zeta}^{\zeta_{\max}} \frac{1}{\zeta}\frac{d}{d\zeta}\left\{\sqrt{\zeta}\,\mathrm{Re}\left[M_{i(\alpha/4),(-3/4)}(i\zeta^2)\right]\right\}d\zeta \right\rangle. \tag{5.30}$$

It is an odd function (since $U_{1(0)}$ is even), which requires $U'_{1(0)}=0$ at $Z=0$

$$B_5 \int_{0}^{\zeta_{\max}} \frac{1}{\zeta}\frac{dD(\zeta)}{d\zeta}d\zeta + B_6 \int_{0}^{\zeta_{\max}} \frac{1}{\zeta}\frac{d}{d\zeta}\left\{\sqrt{\zeta}\,\mathrm{Re}\left[M_{i(\alpha/4),(-3/4)}(i\zeta^2)\right]\right\}d\zeta = 0. \tag{5.31}$$

Eqs. (5.29) and (5.31) give two linear, homogeneous equations for B_5 and B_6. Their determinant must be zero in order to have a non-trivial solution, which gives the equation for the critical buckling load

$$\begin{vmatrix} \int_0^{\zeta_{\max}} D(\zeta)d\zeta & \int_0^{\zeta_{\max}} \sqrt{\zeta}\,\mathrm{Re}\left[M_{i(\alpha/4),(-3/4)}(i\zeta^2)\right]d\zeta \\ \int_0^{\zeta_{\max}} \frac{1}{\zeta}\frac{dD(\zeta)}{d\zeta}d\zeta & \int_0^{\zeta_{\max}} \frac{1}{\zeta}\frac{d}{d\zeta}\left\{\sqrt{\zeta}\,\mathrm{Re}\left[M_{i(\alpha/4),(-3/4)}(i\zeta^2)\right]\right\}d\zeta \end{vmatrix} = 0. \tag{5.32}$$

Its solution $\zeta_{\max}=\zeta_{\max}(\alpha)$ is different from $\zeta_{\max}$ after Eq. (5.20) for the symmetric buckling mode. The critical buckling load is given by Eq. (5.21), but with the new $\zeta_{\max}$ above for the anti-symmetric buckling mode. As shown in Fig. 6, the (normalized) critical buckling load, $\left|\overset{\circ}{P}_{\bar{Z}}\right|(L+L_{island})L^2/(8\sqrt{EI_2C})$, is essentially independent of ν, and is larger for stretching than for compressing. For the island-bridge, mesh structure under stretching along 45° direction, symmetric buckling mode occurs since it gives a small buckling load than the anti-symmetric mode. For compressing along 45° direction, however, both symmetric and anti-symmetric modes may occur since their corresponding buckling loads are very close.

Integration of Eq. (5.30) and the boundary condition $U_{1(0)}|_{Z=L/2}=0$ give

$$\frac{U_{1(0)}}{L} = -\frac{\alpha}{2\zeta_{\max}}\left\langle B_5\left[\zeta\int_{\zeta}^{\zeta_{\max}}\frac{D(\zeta)}{\zeta^2}d\zeta - \frac{\zeta_{\max}-\zeta}{\zeta_{\max}}D(\zeta_{\max})\right] + B_6\left\{\begin{array}{l}\zeta\int_{\zeta}^{\zeta_{\max}}\mathrm{Re}\left[M_{i(\alpha/4),(-3/4)}(i\zeta^2)\right]\frac{1}{\zeta^{3/2}}d\zeta \\ -\frac{\zeta_{\max}-\zeta}{\sqrt{\zeta_{\max}}}\mathrm{Re}\left[M_{i(\alpha/4),(-3/4)}(i\zeta_{\max}^2)\right]\end{array}\right\}\right\rangle. \tag{5.33}$$

The parameter a in Eq. (4.15) is the ratio of maximum displacement to L, i.e., $a=U_{1\max}/L$, which, together with Eq. (5.33), give

$$B_5 D(\zeta_{\max}) + B_6\left\{\sqrt{\zeta_{\max}}\,\mathrm{Re}\left[M_{i(\alpha/4),(-3/4)}(i\zeta_{\max}^2)\right] - \cos\frac{\pi}{8}\right\} = \frac{2\zeta_{\max}}{\alpha}. \tag{5.34}$$

Eqs. (5.29) and (5.34) give two equations to determine B_5 and B_6. Eq. (5.15) then gives $U_{2(0)}$ and $U_{3(0)}$.

The applied strain along $\bar{Z}$ (45°) direction during postbuckling is

$$\varepsilon_{45^\circ} = \frac{U_{1\max}^2}{(L+L_{island})L}\left\{\frac{\alpha}{\zeta_{\max}}\int_0^{\zeta_{\max}}\underline{\left(\frac{d\phi_{(0)}}{d\zeta}\right)^2}d\zeta - 2\zeta_{\max}\int_0^{\zeta_{\max}}\left[\frac{d}{d\zeta}\left(\frac{U_{1(0)}}{L}\right)\right]^2 d\zeta\right\}. \tag{5.35}$$

The maximum bending strain at the onset of buckling is $\varepsilon_{bending}=\overset{\circ}{\beta}{}^{anti}_{bending}h^2/(Lb)$. The maximum bending strain and torsion (shear) strain due to postbuckling are

$$\varepsilon_{bending} = \beta^{anti}_{bending}\frac{h}{L}\sqrt{\frac{L+L_{island}}{L}|\varepsilon_{45^\circ}|}, \tag{5.36}$$

$$\gamma_{torsion} = \beta^{anti}_{torsion}\frac{h}{L}\sqrt{\frac{L+L_{island}}{L}|\varepsilon_{45^\circ}|}. \tag{5.37}$$

Here the coefficients β's are given in Tables 1 and 2, and are essentially independent of the Poisson's ratio ν. Without accounting for the 4th power of displacement, postbuckling for stretching along 45° could not be studied because $\varepsilon_{45^\circ}<0$ in Eq. (5.35), and the maximum bending and shear strains would be significantly overestimated for compressing along 45°.

Fig. 4c shows the symmetric and anti-symmetric buckling modes in Sections 5.4 and 5.5, respectively. The applied strain is $\varepsilon_{45^\circ} = \pm 10\% \cdot L/(L+L_{island})$ (for both stretching and compressing), and $C/EI_2 = 1.57$. The buckling mode for the anti-symmetric appears to be rather similar to the experimentally observed buckling profile in Fig. 1c for the stretching case.

5.6. Maximum strains

5.6.1. 45°-Direction stretching

Comparison of Eqs. (5.36) and (5.37) with Eqs. (5.24) and (5.25), together with Tables 1 and 2, suggest that the symmetric buckling mode always gives smaller bending and torsion strains than anti-symmetric buckling. The maximum bending and torsion strains are then given by

$$\varepsilon_{bending} \approx 6.5\frac{h}{L}\sqrt{\frac{L+L_{island}}{L}|\varepsilon_{45^\circ}|}, \quad \gamma_{torsion} \approx 10\frac{h}{L}\sqrt{\frac{L+L_{island}}{L}|\varepsilon_{45^\circ}|}, \tag{5.38}$$

where the bending strain at the onset of buckling is neglected, and the coefficient β's for $\nu = 0.3$ are used since their variations are small ($\sim 5\%$) in Tables 1 and 2. These maximum strains are not reached at the same point in the bridge. The maximum principal strain is the same as the maximum bending strain, i.e.

$$\varepsilon_{\max} \approx 6.5\frac{h}{L}\sqrt{\frac{L+L_{island}}{L}|\varepsilon_{45^\circ}|}.$$

5.6.2. 45°-Direction compressing

Eqs. (5.24), (5.25), (5.36) and (5.37), together with Tables 1 and 2, suggest that the symmetric buckling mode gives larger bending strain and but smaller torsion strain than anti-symmetric buckling. The maximum bending and torsion strains can then be bounded as

$$\varepsilon_{bending} \le 5.5\frac{h}{L}\sqrt{\frac{L+L_{island}}{L}|\varepsilon_{45^\circ}|}, \quad \gamma_{torsion} \le 8.6\frac{h}{L}\sqrt{\frac{L+L_{island}}{L}|\varepsilon_{45^\circ}|}. \tag{5.39}$$

The maximum principal strain is the same as the maximum bending strain, i.e.

$$\varepsilon_{\max} \le 5.5\frac{h}{L}\sqrt{\frac{L+L_{island}}{L}|\varepsilon_{45^\circ}|}.$$

For Euler buckling, Song et al. (2009) used both analytical and finite element methods to show that the maximum strain in the island is much smaller than that in the bridge, even at the stress and strain concentration at the island-bridge interface. This is also expected to hold also for the complex buckling modes in the present study.

6. Concluding remarks

(i) All terms up to the 4th power of displacements in the potential energy are necessary in the postbuckling analysis (Koiter, 1945). The existing postbuckling analyses, however, are accurate only to the 2nd power of displacements in the potential energy since they assume a linear displacement–curvature relation.

(ii) A systematic method is established for postbuckling analysis of beams that may involve complex buckling modes (e.g., lateral buckling under arbitrary loading). It avoids complex geometric analysis of deformation for postbuckling (Timoshenko and Gere, 1961), and accounts for all terms up to the 4th power of displacements in the potential energy.

(iii) The lateral buckling mode of an island-bridge, mesh structure subject to shear (or twist), which is used in stretchable electronics, involves the Bessel Function of the first kind. Simple, analytical expressions are obtained for the critical load at the onset of buckling in Eqs. (4.27) and (4.40), and for the maximum bending and torsion strains during postbuckling in Eqs. (4.30), (4.31), (4.45) and (4.46).

(iv) Buckling of the island-bridge, mesh structure subject to diagonal stretching (and compressing) involves the Whittaker M function. Simple, analytical expressions are obtained for the maximum bending, torsion (shear) and principal strains during postbuckling in Eq. (5.38).

Acknowledgments

The authors acknowledge support from NSF Grant nos. ECCS-0824129 and OISE-1043143, and DOE, Division of Materials Sciences Grant no.DE-FG02-07ER46453. The support from NSFC (Grant no. 11172146) and the Ministry of Education, China is also acknowledged.

Appendix A

The 3rd order terms in the direction cosines a_{ij} and curvatures κ_i are

$$\begin{cases} a_{11}^{(3)} = -\frac{1}{2}\phi U_1' U_2' - \phi\psi^{(2)} + U_1'^2 U_3', \quad a_{12}^{(3)} = \frac{1}{4}\phi(U_1'^2 - U_2'^2) + U_1' U_2' U_3' + \psi^{(3)}, \\ a_{13}^{(3)} = \frac{1}{2}\phi^2 U_1' + \phi U_2' U_3' - \psi^{(2)} U_2' - U_1'\left[U_3'^2 - \frac{1}{2}(U_1'^2 + U_2'^2)\right], \\ a_{21}^{(3)} = \frac{1}{4}\phi(U_1'^2 - U_2'^2) + U_1' U_2' U_3' - \psi^{(3)}, \quad a_{22}^{(3)} = \frac{1}{2}\phi U_1' U_2' - \phi\psi^{(2)} + U_2'^2 U_3', \\ a_{23}^{(3)} = \frac{1}{2}\phi^2 U_2' - \phi U_1' U_3' + \psi^{(2)} U_1' - U_2'\left[U_3'^2 - \frac{1}{2}(U_1'^2 + U_2'^2)\right], \\ a_{31}^{(3)} = U_1'\left[U_3'^2 - \frac{1}{2}(U_1'^2 + U_2'^2)\right], \quad a_{32}^{(3)} = U_2'\left[U_3'^2 - \frac{1}{2}(U_1'^2 + U_2'^2)\right], \quad a_{33}^{(3)} = U_3'(U_1'^2 + U_2'^2), \end{cases} \tag{A.1}$$

$$\begin{cases} \hat{\kappa}_1^{(3)} = \psi^{(2)} U_1'' + \frac{1}{2}\phi^2 U_2'' - \phi(U_1'' U_3' + U_1' U_3'') + U_2''\left(\frac{1}{2}U_1'^2 + U_2'^2 - U_3'^2\right) + \frac{1}{2}U_1'' U_1' U_2' - 2U_3'' U_2' U_3', \\ \hat{\kappa}_2^{(3)} = \psi^{(2)} U_2'' - \frac{1}{2}\phi^2 U_1'' - \phi(U_2'' U_3' + U_2' U_3'') - U_1''\left(\frac{1}{2}U_2'^2 + U_1'^2 - U_3'^2\right) - \frac{1}{2}U_2'' U_1' U_2' + 2U_3'' U_1' U_3', \\ \hat{\kappa}_3^{(3)} = 0, \end{cases} \tag{A.2}$$

where

$$\psi^{(3)} = \int_0^Z \left\{ -\frac{1}{2}\phi'\phi^2 - \frac{1}{4}\left[\phi(U_1'^2 + U_2'^2)\right]' + (U_1'' U_2' - U_1' U_2'')U_3' \right\} dZ.$$

The orthogonal condition before Eq. (3.21) can be proven as

$$\begin{aligned} \int_{-L/2}^{L/2} \left(U_{1(1)}'' + \frac{\overset{\circ}{P}}{EI_2} U_{1(1)}\right)'' U_{1(0)} dZ &= \int_{-L/2}^{L/2} \left[\left(U_{1(1)}'' + \frac{\overset{\circ}{P}}{EI_2} U_{1(1)}\right)'' U_{1(0)} - \left(U_{1(0)}'' + \frac{\overset{\circ}{P}}{EI_2} U_{1(0)}\right)'' U_{1(1)}\right] dZ \\ &= (U_{1(1)}''' U_{1(0)} - U_{1(1)} U_{1(0)}'')\Big|_{Z=-L/2}^{L/2} - (U_{1(1)}'' U_{1(0)}' - U_{1(1)}' U_{1(0)}'')\Big|_{Z=-L/2}^{L/2} + \frac{\overset{\circ}{P}}{EI_2}(U_{1(1)}' U_{1(0)} - U_{1(1)} U_{1(0)}')\Big|_{Z=-L/2}^{L/2} = 0. \end{aligned} \tag{A.3}$$

The function D in Eq. (5.27) is given by

$$D(\zeta) = T_1(\zeta) \int_{\zeta_1}^{\zeta} \frac{T_2(\zeta)}{\frac{dT_1(\zeta)}{d\zeta} T_2(\zeta) - T_1(\zeta)\frac{dT_2(\zeta)}{d\zeta}} d\zeta - T_2(\zeta) \int_0^{\zeta} \frac{T_1(\zeta)}{\frac{dT_1(\zeta)}{d\zeta} T_2(\zeta) - T_1(\zeta)\frac{dT_2(\zeta)}{d\zeta}} d\zeta, \tag{A.4}$$

where

$$T_1(\zeta) = \sqrt{\zeta}\,\mathrm{Re}[M_{i(\alpha/4),(3/4)}(i\zeta^2)], \quad T_2(\zeta) = \sqrt{\zeta}\,\mathrm{Re}[M_{i(\alpha/4),(-3/4)}(i\zeta^2)], \tag{A.5}$$

which have the limits

$$T_1(\zeta) = \zeta^3 \cos\frac{5\pi}{8}\left[1 + \frac{\alpha}{10}\zeta^2 + O(\zeta^4)\right] \quad \text{and} \quad T_2(\zeta) = \cos\frac{\pi}{8}\left[1 - \frac{\alpha}{2}\zeta^2 + O(\zeta^4)\right] \quad \text{as} \quad \zeta \to 0.$$

The lower limit of the 1st integral ζ_1 in Eq. (A.4) is determined from

$$\lim_{\zeta\to 0} \frac{d}{d\zeta}\left[\zeta \int_{\zeta_1}^{\zeta} \frac{T_2(\zeta)}{\frac{dT_1(\zeta)}{d\zeta} T_2(\zeta) - T_1(\zeta)\frac{dT_2(\zeta)}{d\zeta}} d\zeta\right] = 0. \tag{A.6}$$

References

Bowden, N., Brittain, S., Evans, A.G., Hutchinson, J.W., Whitesides, G.M., 1998. Spontaneous formation of ordered structures in thin films of metals supported on an elastomeric polymer. Nature 393, 146–149.

Budiansky, B., 1973. Theory of buckling and postbuckling behavior of elastic structures. Adv. Appl. Mech. 14, 1–65.

Crawford, G.P., 2005. Flexible Flat Panel Display Technology. John Wiley & Sons, Ltd., New York.

Gradshteyn, I.S., Ryzhik, I.M., 2007. Table of Integrals, Series and Products. Academic Press, London.

Jin, H.C., Abelson, J.R., Erhardt, M.K., Nuzzo, R.G., 2004. Soft lithographic fabrication of an image sensor array on a curved substrate. J. Vac. Sci. Technol. B 22, 2548–2551.

Jung, I., Xiao, J., Malyarchuk, V., Lu, C., Li, M., Liu, Z., Yoon, J., Huang, Y., Rogers, J.A., 2011. Dynamically tunable hemispherical electronic eye camera system with adjustable zoom capability. Proc. Nat. Acad. Sci. USA 108, 1788–1793.

Kim, D.-H., Ahn, J.-H., Choi, W.M., Kim, H.-S., Kim, T.-H., Song, J., Huang, Y.Y., Liu, Z., Lu, C., Rogers, J.A., 2008a. Stretchable and foldable silicon integrated circuits. Science 320, 507–511.

Kim, D.-H., Lu, N., Ghaffari, R., Kim, Y.-S., Lee, S.P., Xu, L., Wu, J., Kim, R.-H., Song, J., Liu, Z., Viventi, J., de Graff, B., Elolampi, B., Mansour, M., Slepian, M.J., Hwang, S., Moss, J.D., Won, S.-M., Huang, Y., Litt, B., Rogers, J.A., 2011a. Materials for multifunctional balloon catheters with capabilities in cardiac electrophysiological mapping and ablation therapy. Nat. Mater. 10, 316–323.

Kim, D.-H., Lu, N., Ma, R., Kim, Y.-S., Kim, R.-H., Wang, S., Wu, J., Won, S.M., Tao, H., Islam, A., Yu, K.J., Kim, T.-i., Chowdhury, R., Ying, M., Xu, L., Li, M., Chung, J.A., Keum, H., McCormick, M., Liu, P., Zhang, Y.-W., Omenetto, F.G., Huang, Y., Coleman, T., Rogers, J.A., 2011b. Epidermal electronics. Science 333, 838–843.

Kim, D.-H., Song, J., Choi, W.M., Kim, H.-S., Kim, R.-H., Liu, Z., Huang, Y.Y., Hwang, K.-C., Zhang, Y.-w., Rogers, J.A., 2008b. Materials and noncoplanar mesh designs for integrated circuits with linear elastic responses to extreme mechanical deformations. Proc. Nat. Acad. Sci. USA 105, 18675–18680.

Kim, D.-H., Viventi, J., Amsden, J.J., Xiao, J., Vigeland, L., Kim, Y.-S., Blanco, J.A., Panilaitis, B., Frechette, E.S., Contreras, D., Kaplan, D.L., Omenetto, F.G., Huang, Y., Hwang, K.-C., Zakin, M.R., Litt, B., Rogers, J.A., 2010a. Dissolvable films of silk fibroin for ultrathin conformal bio-integrated electronics. Nat. Mater. 9, 511–517.

Kim, R.-H., Kim, D.-H., Xiao, J., Kim, B.H., Park, S.-I., Panilaitis, B., Ghaffari, R., Yao, J., Li, M., Liu, Z., Malyarchuk, V., Kim, D.G., Le, A.-P., Nuzzo, R.G., Kaplan, D.L., Omenetto, F.G., Huang, Y., Kang, Z., Rogers, J.A., 2010b. Waterproof AlInGaP optoelectronics on stretchable substrates with applications in biomedicine and robotics. Nat. Mater. 9, 929–937.

Ko, H.C., Stoykovich, M.P., Song, J., Malyarchuk, V., Choi, W.M., Yu, C.-J., Geddes III, J.B., Xiao, J., Wang, S., Huang, Y., Rogers, J.A., 2008. A hemispherical electronic eye camera based on compressible silicon optoelectronics. Nature 454, 748–753.

Koiter, W.T., 1945. On the stability of elastic equilibrium (in Dutch). Thesis. Delft Univ., H.J. Paris, Amsterdam; English transl. (a) NASA TT-F10.833 (1967). (b) AFFDL-TR-70-25 (1970).

Koiter, W.T., 1963. Elastic stability and post-buckling behavior. In: Langer, R.E. (Ed.), Nonlinear Problems, Univ. Wisconsin Pr., pp. 257–275.

Koiter, W.T., 2009. In: van der Heijden, A.M. (Ed.), Elastic stability of solids and structures, Cambridge University Press, New York, USA.

Love, A.E.H., 1927. A Treatise on the Mathematical Theory of Elasticity. Dover, New York, USA.

Mannsfeld, S.C.B., Tee, B.C.K., Stoltenberg, R.M., Chen, C.V.H.H., Barman, S., Muir, B.V.O., Sokolov, A.N., Reese, C., Bao, Z., 2010. Highly sensitive flexible pressure sensors with microstructured rubber dielectric layers. Nat. Mater. 9, 859–864.

Nathan, A., Park, B., Sazonov, A., Tao, S., Chan, I., Servati, P., Karim, K., Charania, T., Striakhilev, D., Ma, Q., Murthy, R.V.R., 2000. Amorphous silicon detector and thin film transistor technology for large-area imaging of X-rays. Microelectron. J. 31, 883–891.

Park, S.-I., Xiong, Y., Kim, R.-H., Elvikis, P., Meitl, M., Kim, D.-H., Wu, J., Yoon, J., Yu, C.-J., Liu, Z., Huang, Y., Hwang, K.-c., Ferreira, P., Li, X., Choquette, K., Rogers, J.A., 2009. Printed assemblies of inorganic light-emitting diodes for deformable and semitransparent displays. Science 325, 977–981.

Rogers, J.A., Someya, T., Huang, Y., 2010. Materials and mechanics for stretchable electronics. Science 327, 1603–1607.

Someya, T., Sekitani, T., Iba, S., Kato, Y., Kawaguchi, H., Sakurai, T., 2004. A large-area, flexible pressure sensor matrix with organic field-effect transistors for artificial skin applications. Proc. Nat. Acad. Sci. USA 101, 9966–9970.

Song, J., Huang, Y., Xiao, J., Wang, S., Hwang, K.C., Ko, H.C., Kim, D.H., Stoykovich, M.P., Rogers, J.A., 2009. Mechanics of noncoplanar mesh design for stretchable electronic circuits. J. Appl. Phys., 105.

Takei, K., Takahashi, T., Ho, J.C., Ko, H., Gillies, A.G., Leu, P.W., Fearing, R.S., Javey, A., 2010. Nanowire active-matrix circuitry for low-voltage macroscale artificial skin. Nat. Mater. 9, 821–826.

Timoshenko, S.P., Gere, J.M., 1961. In: Theory of Elastic Stability, 2nd Edition. McGraw-Hill, New York, USA.

Viventi, J., Kim, D.-H., Moss, J.D., Kim, Y.-S., Blanco, J.A., Annetta, N., Hicks, A., Xiao, J., Huang, Y., Callans, D.J., Rogers, J.A., Litt, B., 2010. A conformal, bio-interfaced class of silicon electronics for mapping cardiac electrophysiology. Sci. Translational Med. 2 24ra22.

von Karman, T., Tsien, H.S., 1941. The buckling of thin cylindrical shells under axial compression. J. Aeronaut. Sci. 8, 303.

Yoon, J., Baca, A.J., Park, S.-I., Elvikis, P., Geddes III, J.B., Li, L., Kim, R.H., Xiao, J., Wang, S., Kim, T.-H., Motala, M.J., Ahn, B.Y., Duoss, E.B., Lewis, J.A., Nuzzo, R.G., Ferreira, P.M., Huang, Y., Rockett, A., Rogers, J.A., 2008. Ultrathin silicon solar microcells for semitransparent, mechanically flexible and microconcentrator module designs. Nat. Mater. 7, 907–915.